This Supplementary Information was republished on 11th March 2021. The direction of the reaction arrows between the open and closed form of the photoacid in Figure S32 was previously incorrect, and unrelated references S12-14 about crystallographic work were listed. The corrected figure is now shown, and the previous references S12-14 have been removed.

Electronic Supplementary Material

Light-induced assembly and disassembly of polymers with Pd_nL_{2n}-type network junctions

Ru-Jin Li, Cristian Pezzato, Cesare Berton, and Kay Severin*

Institut des Sciences et Ingénierie Chimiques, École Polytechnique Fédérale de Lausanne (EPFL), 1015 Lausanne, Switzerland

Table of Contents

1 General

All chemicals were obtained from commercial sources and used without further purification unless stated otherwise. The ligands **L1'**,[S1] **L2'**,[S2] **L3'**,[S3] **L4'**,[S4] **L5**[S5] (structures are depicted below), **L1'-OH**,[S6] **L2'-OH**,[S7] **L3'-OH**,[S7] the cages $[Pd_2(\mathbf{L1'})_4](BF_4)_4$,[S1] $[Pd_6(\mathbf{L5})_{12}](BF_4)_{12}$,[S5] the carbene complex $[PdBr_2(i\text{Pr}_2\text{-bimy})]_2$[S8] for determining the HEP, poly(ethylene glycol) (average Mn 4600) bis(tosylate),[S9] and 1-(2-hydroxyethyl)-2,3,3-trimethyl-3H-indolium bromide[S10] were prepared accoring to literature procedures. Solution NMR spectra were obtained on a Bruker DRX (400 MHz). Magic-angle spinning solid-state nuclear magnetic resonance (^{1}H MAS NMR) spectra of the gel samples were were performed using a 400 MHz narrow boremagnet equipped with an Avance Neo Hybrid console and a 3.2 mm cross-polarization variable temperature magic angle spinning probe (H128922/0004). Samples were analyzed at a spin rate of 8 kHz for ^{1}H measurements and referenced using CH_3CN/DMSO solvent with respect to TMS at 0 ppm. High resolution mass spectra were acquired using a hybrid ion trap-Orbitrap Fourier transform mass spectrometer, Orbitrap Elite (Thermo Scientific) equipped with a TriVersa Nanomate (Advion) nano-electrospray ionization source. Frequency sweep rheology experiments were recordeded on a TA Instruments Discovery Hybrid Rheometer HR-2 with a 8 mm (radius) parallel-plate geometry. The rheometer was outfitted with an active temperature control system with an environmental enclosure for temperature control. A parallel-plate geometry (radius 8 mm) was used and coupled with a bottom plate, with the typical gap of 1.00 mm between the two plates. Frequency sweep experiments were performed from 0.1 rad s^{-1} to 100 rad s^{-1} at 0.5% strain. The loaded gel samples were immersed in mineral oil to reduce solvent evaporation. The irradiations were performed with a 90 W LED at ~456 nm from Kessil A360W-E TUNA BLUE. UV-Vis spectra were recorded on an Agilent Cary 60 UV-Visible spectrophotometer. Scanning electron microscopy (SEM) was performed on GeminiSEM 300.

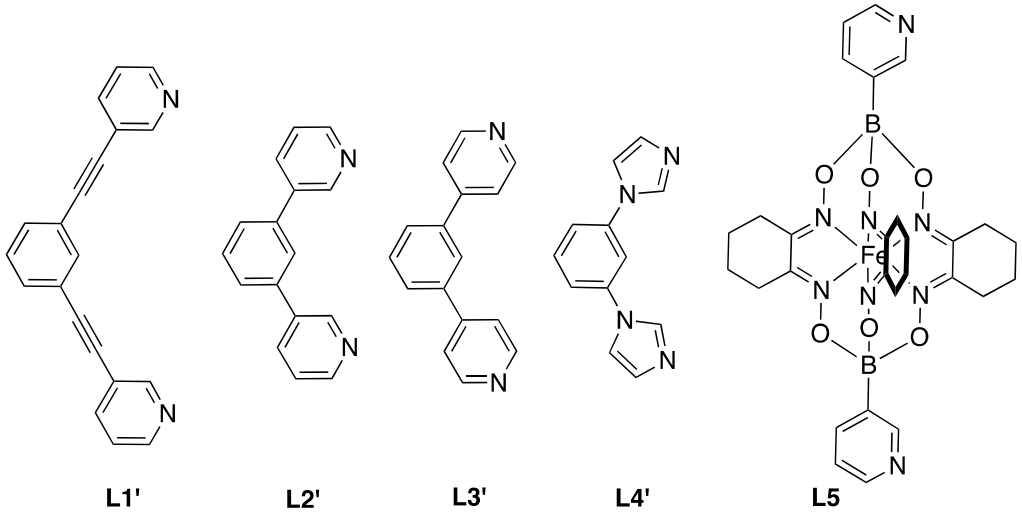

Structures of the ligands **L1'**–**L4'** and **L5**.

2 Synthesis

2.1 Synthesis of the ligands **L1**–**L4**

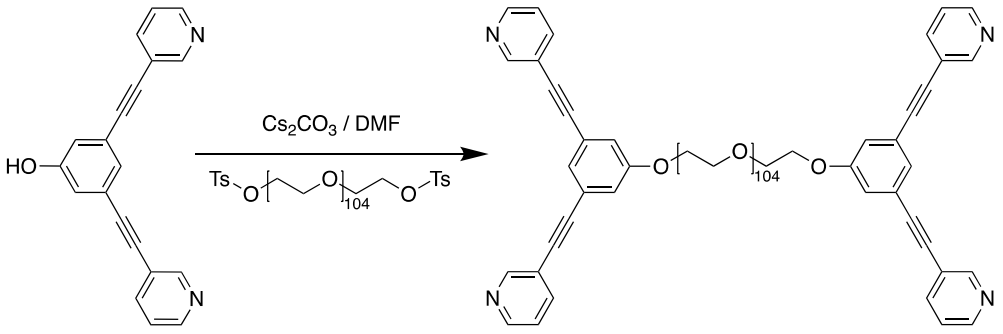

L1'-OH **L1**

A mixture of **L1'-OH** (92 mg, 0.31 mmol) and Cs_2CO_3 (151 mg, 0.47 mmol) was combined in a 25 mL Schlenk tube. After vacuum/backfilling with N_2 for three times, anhydrous DMF (8 mL) was added. The mixture was stirred at 80 ºC for 1 h, before poly(ethylene glycol) (average Mn 4600) bis(tosylate) (0.5 g, 0.10 mmol) was added. The mixture was allowed to stir at 80 ºC for one day. The reaction was cooled to room temperature, quenched with water, extracted with DCM for three times, washed with water and brine, dried over Na_2SO_4, and the solvent was removed under reduced pressure. The crude product was dissolved in a minimum amount of ethyl acetate and precipitated with cold diethyl ether. The resulting solid precipitate was collected via filtration and washed with additional ether. The precipitation procedure was repeated 4 times, giving a white grey powder (**L1**) (288 mg, 56%). ^{1}H NMR (400 MHz, CD_3CN) δ 8.75 (s, 4H), 8.57 (d, J = 4.8 Hz, 4H), 7.95 – 7.86 (m, 4H), 7.39 (dd, J = 7.9, 4.8 Hz, 4H), 7.35 (s, 2H), 7.19 (d, J = 1.3 Hz, 4H), 4.17 (d, J = 4.7 Hz, 4H), 3.80 (t, J = 4.5 Hz, 4H), δ 3.71 (d, J = 5.3 Hz, 2H), 3.64 (d, J = 5.3 Hz, 4H), 3.55 (s, 440H) 3.37 (d, J = 5.1 Hz, 2H).

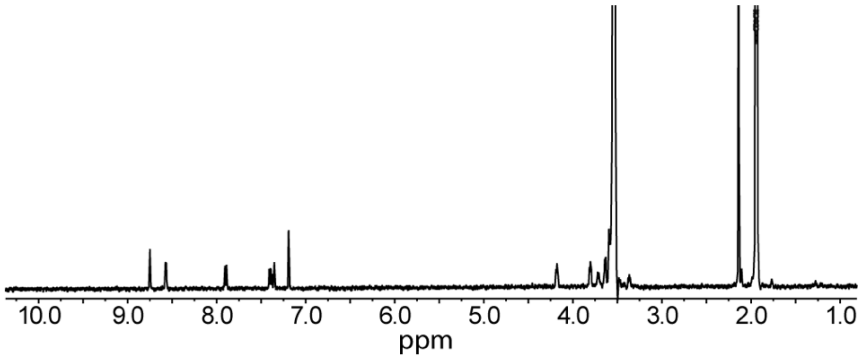

Figure S1. ^{1}H NMR (400 MHz, CD_3CN) spectrum of ligand **L1**.

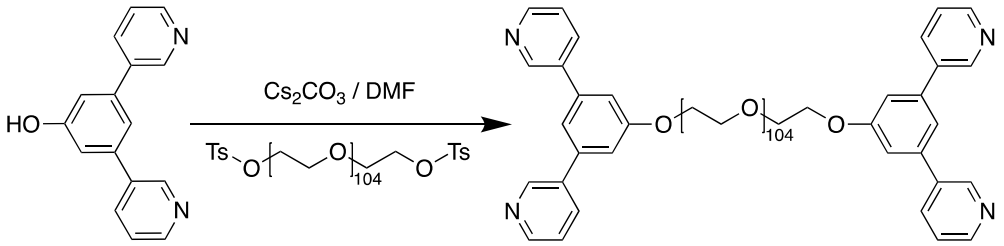

L2'-OH **L2**

A mixture of **L2'-OH** (154 mg, 0.62 mmol) and Cs_2CO_3 (302 mg, 0.93 mmol) was combined in a 25 mL Schlenk tube. After vacuum/backfilling with N_2 for three times, anhydrous DMF (12 mL) was added. The mixture was stirred at 80 ºC for 1 h, before poly(ethylene glycol) (average Mn 4600) bis(tosylate) (1.0 g, 0.20 mmol) was added. The mixture was allowed to stir at 80 ºC for one day. The reaction was cooled to room temperature, quenched with water, extracted with DCM for three times, washed with water and brine, dried over Na_2SO_4 and the solvent was removed under reduced pressure. The crude product was dissolved in a minimum amount of ethyl acetate and precipitated in cold diethyl ether. The resulting solid precipitate was collected via filtration and washed with additional ether. The precipitation procedure was repeated 4 times, giving a white powder (**L2**) (730 mg, 72%). ^{1}H NMR (400 MHz, CD_3CN) δ 8.95 (d, *J* = 2.4 Hz, 4H), 8.59 (dd, *J* = 4.8, 1.6 Hz, 4H), 8.08 (d, *J* = 8.1 Hz, 4H), 7.54 (s, 2H), 7.44 (ddd, *J* = 7.9, 4.8, 0.9 Hz, 4H), 7.27 (d, *J* = 1.5 Hz, 4H), 4.32 – 4.25 (m, 4H), 3.87 – 3.81 (m, 4H), 3.75 – 3.68 (m, 2H), 3.65 (dt, *J* = 3.9, 2.7 Hz, 4H), 3.63 – 3.44 (m, 490H), 3.37 (dd, *J* = 5.8, 3.6 Hz, 2H).

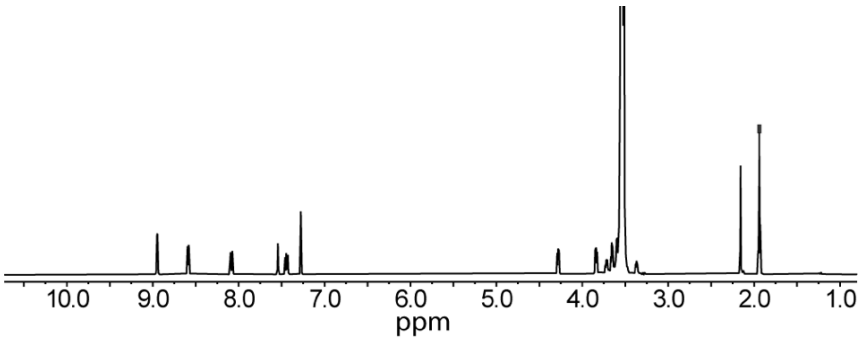

Figure S2. ^{1}H NMR (400 MHz, CD_3CN) spectrum of ligand **L2**.

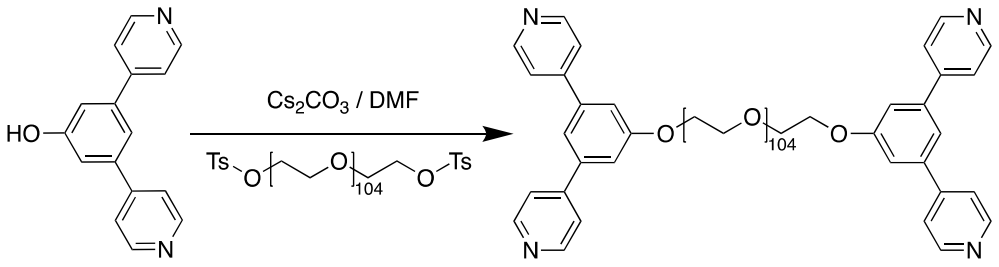

A mixture of **L3'-OH** (154 mg, 0.62 mmol) and Cs_2CO_3 (302 mg, 0.93 mmol) was combined in a 25 mL Schlenk tube. After vacuum/backfilling with N_2 for three times, anhydrous DMF (12 mL) was added. The mixture was stirred at 80 ºC for 1 h, before 1.0 g poly(ethylene glycol) (average Mn 4600) bis(tosylate) (0.20 mmol) was added. The mixture was allowed to stir at 80 ºC for one day. The reaction was cooled to room temperature, quenched with water, extracted with DCM for three times, washed with water and brine, dried over Na_2SO_4 and the solvent was removed under reduced pressure. The crude product was dissolved in a minimum amount of ethyl acetate and precipitated in cold diethyl ether. The resulting solid precipitate was collected via filtration and washed with additional ether. The precipitation procedure was repeated 4 times, giving a white grey powder (**L3**) (678 mg, 67%). ^{1}H NMR (400 MHz, CD_3CN) δ 8.69 – 8.63 (m, 8H), 7.74 – 7.68 (m, 8H), 7.65 (t, *J* = 1.6 Hz, 2H), 7.37 (d, *J* = 1.5 Hz, 4H), 4.32 – 4.26 (m, 4H), 3.87 – 3.81 (m, 4H), 3.72 (dd, *J* = 5.5, 4.0 Hz, 2H), 3.68 – 3.63 (m, 4H), 3.55 (s, 480H), 3.37 (t, *J* = 4.7 Hz, 2H).

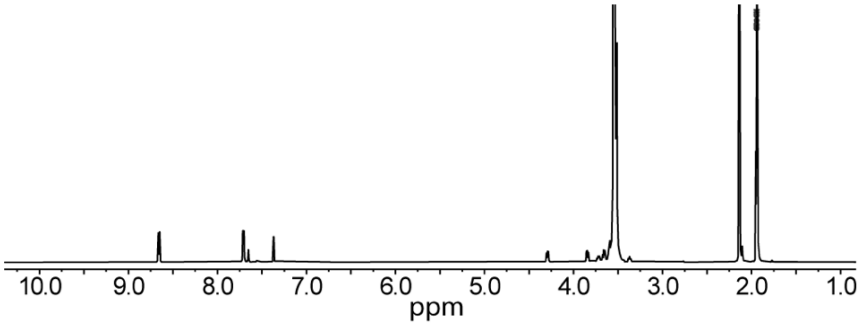

Figure S3. ^{1}H NMR (400 MHz, CD_3CN) spectrum of ligand **L3**.

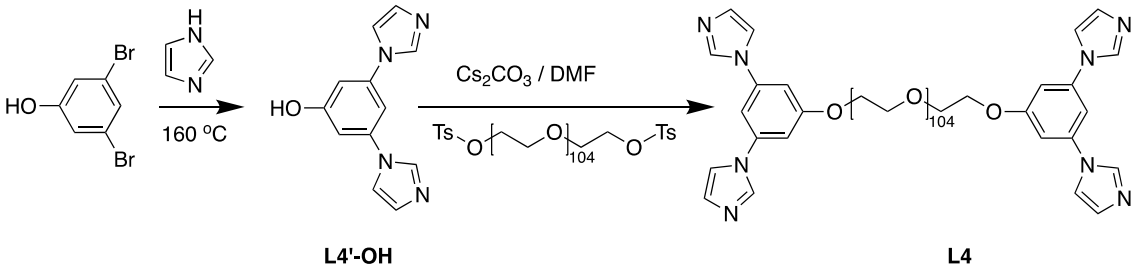

L4'-OH **L4**

L4'-OH: A mixture of 3,5-dibromophenol (0.5 g, 1.98 mmol) and 1*H*-imidazole (0.5 g, 7.35 mmol) was combined in a 25 mL Schlenk tube. After vacuum/backfilling with N_2 for three times, the mixture was gradually heated up to 100 °C and kept for 3 h, later increased to 150 °C overnight. The reaction was cooled to room temperature, quenched with water, extracted with DCM for two times, washed with water for three times and brine, dried over Na_2SO_4, and the solvent was removed under reduced pressure. A light green-white powder (**L4'-OH**) was obtained (301 mg, 64%). ^{1}H NMR (400 MHz, DMSO) δ 10.39 (s, 1H), 8.38 (s, 2H), 7.85 (s, 2H), 7.40 (s, 1H), 7.30 – 7.06 (m, 2H), 6.99 (s, 2H). ^{13}C NMR (101 MHz, DMSO) δ 160.09, 139.46, 130.59, 119.06, 106.02, 103.64. ESI-MS: *m/z* calculated for C12H11N4O $[M+H]^+$ 227.09, found 227.09.

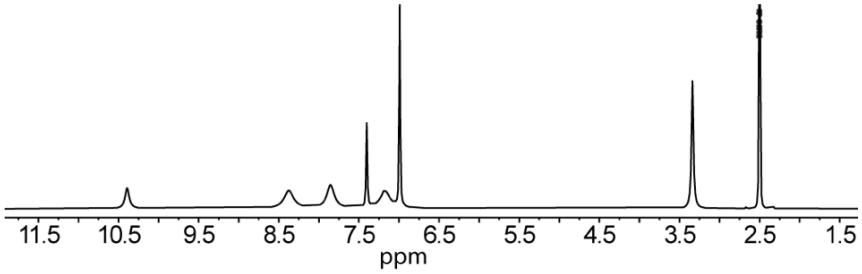

Figure S4. ^{1}H NMR (400 MHz, d_6-DMSO) spectrum of **L4'-OH**.

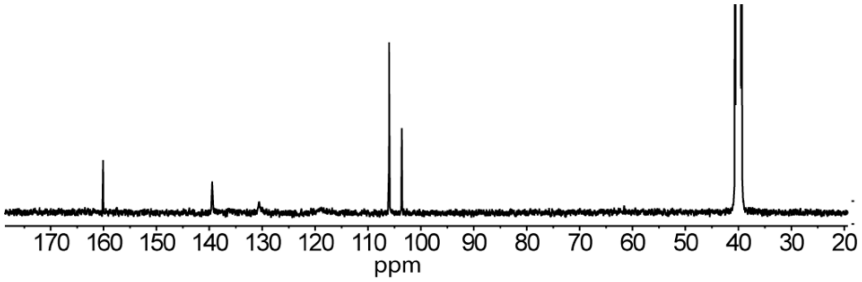

Figure S5. ^{13}C NMR (101 MHz, d_6-DMSO) spectrum of **L4'-OH**.

L4: A mixture of **L4'-OH** (154 mg, 0.62 mmol) and Cs_2CO_3 (302 mg, 0.93 mmol) was combined in a 25 mL Schlenk tube. After vacuum/backfilling with N_2 for three times, anhydrous DMF (12 mL) was added. The mixture was stirred at 80 ºC for 1 h, before poly(ethylene glycol) (average Mn 4600) bis(tosylate) (1.0 g, 0.20 mmol) was added. The mixture was allowed to stir at 80 ºC for one day. The reaction was cooled to room temperature, quenched with water, extracted with DCM for three times, washed with water and brine, dried over Na_2SO_4 and the solvent was removed under reduced pressure. The crude product was dissolved in a minimum amount of ethyl acetate and precipitated in cold diethyl ether. The resulting solid precipitate was collected via filtration and washed with additional ether. The precipitation procedure was repeated 4 times, giving a white powder (**L4**) (775 mg,

78%). ^{1}H NMR (400 MHz, CD_3CN) δ 8.06 (s, 4H), 7.57 (s, 4H), 7.30 (t, J = 1.9 Hz, 2H), 7.13 (s, 4H), 7.10 (d, J = 1.9 Hz, 4H), 4.29 – 4.23 (m, 4H), 3.86 – 3.80 (m, 4H), 3.75 – 3.68 (m, 2H), 3.67 – 3.61 (m, 4H), 3.55 (d, J = 3.2 Hz, 460H), 3.37 (t, J = 4.7 Hz, 2H).

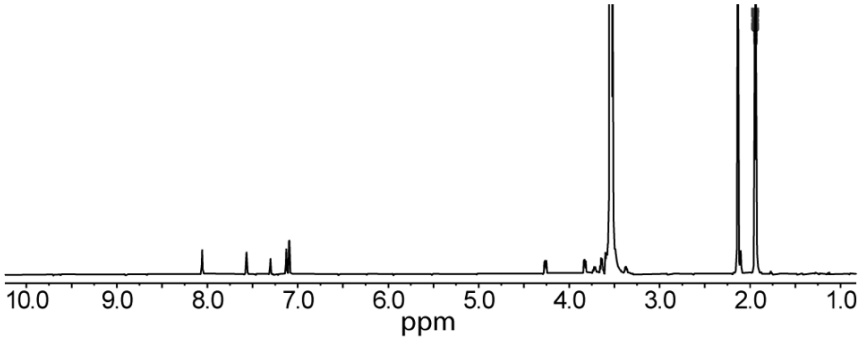

Figure S6. ^{1}H NMR (400 MHz, CD_3CN) spectrum of ligand **L4**.

2.2 Synthesis of cages

2.2.1 Synthesis of $[Pd_2(\mathbf{L2'})_4](BF_4)_4$ & $[Pd_2(\mathbf{L2'})_3X_2](BF_4)_4$

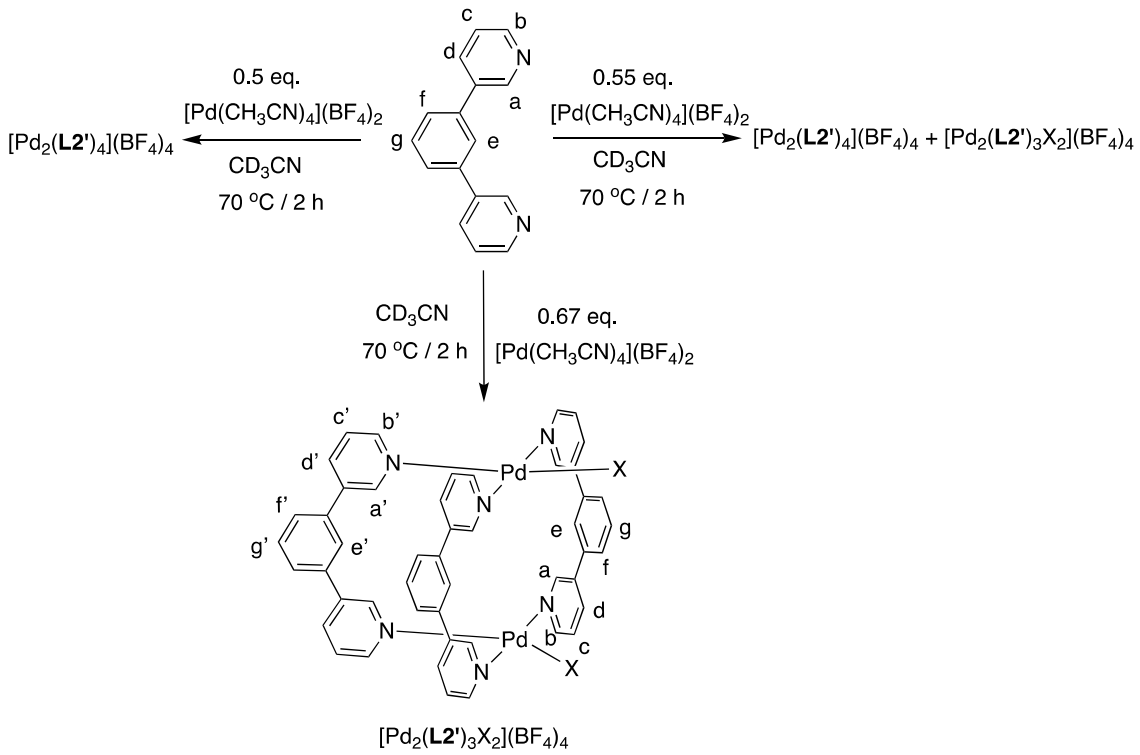

The cage compound $[Pd_2(\mathbf{L2'})_4](BF_4)_4$ was synthesized in quantitative yield by stiring a mixture of ligand **L2'** (9 μmol, 200 μL of a 45 mM stock solution of **L2'** in CD_3CN) and $[Pd(CH_3CN)_4](BF_4)_2$ (4.5 μmol, 150 μL of a 30 mM stock solution in CD_3CN) in 650 μL CD_3CN at 70 °C for 2 h to give 1000 μL of a 2.25 mM solution of cage $[Pd_2(\mathbf{L2'})_4](BF_4)_4$. ^{1}H NMR (400 MHz, CD_3CN) δ 9.82 (s, 8H), 9.03 (d, *J* = 5.7 Hz, 8H), 8.51 (s, 4H), 8.19 (dd, *J* = 8.1, 1.7 Hz, 4H), 7.68 – 7.59 (m, 16H), 7.56 (q, *J* = 7.8, 6.4 Hz, 4H). ^{13}C NMR (101 MHz, CD_3CN) δ 151.74, 150.80, 140.76, 140.33, 137.38, 131.37, 129.55, 128.29, 128.03. When mixing ligand **L2'** (9 μmol, 200 μL of a 45 mM stock solution of **L2'** in CD_3CN) with 0.55 equiv. (slightly excess) of $[Pd(CH_3CN)_4](BF_4)_2$ (4.95 μmol, 165 μL of a 30 mM stock solution in CD_3CN) in 650 μL CD_3CN at 70 °C for 2 h, however, offered a mixture of cage $[Pd_2(\mathbf{L2'})_4](BF_4)_4$ and bowl compound $[Pd_2(\mathbf{L2'})_3X_2](BF_4)_4$ (X is most likely acetonitrile).

The clean formation of the bowl-shaped compound $[Pd_2(\mathbf{L2'})_3X_2](BF_4)_4$ was observed upon equilibration (70 °C for 2 h) of a 3:2 mixture of ligand **L2'** (9 μmol, 200 μL of a 45 mM stock solution of **L2'** in CD_3CN) and $[Pd(CH_3CN)_4](BF_4)_2$ (6 μmol, 200 μL of a 30 mM stock solution in CD_3CN) in 600 μL CD_3CN. ^{1}H NMR (400 MHz, CD_3CN) δ 9.89 (d, *J* = 2.1 Hz, 4H), 9.35 (d, *J* = 2.0 Hz, 2H), 9.09 – 9.04 (m, 2H), 8.91 (dd, *J* = 5.9, 1.3 Hz, 4H), 8.52 (s, 2H), 8.35 (dt, *J* = 8.3, 1.5 Hz, 4H), 8.28 – 8.20 (m, 2H), 8.13 (s, 1H), 7.83 – 7.48 (m, 15H). ^{13}C NMR (101 MHz, CD_3CN) δ 151.45, 151.37, 151.27, 149.63, 140.67, 140.38, 140.30, 140.25, 137.15, 136.32, 131.67, 131.62, 129.64, 129.37, 128.70, 128.18, 127.26, 126.30.

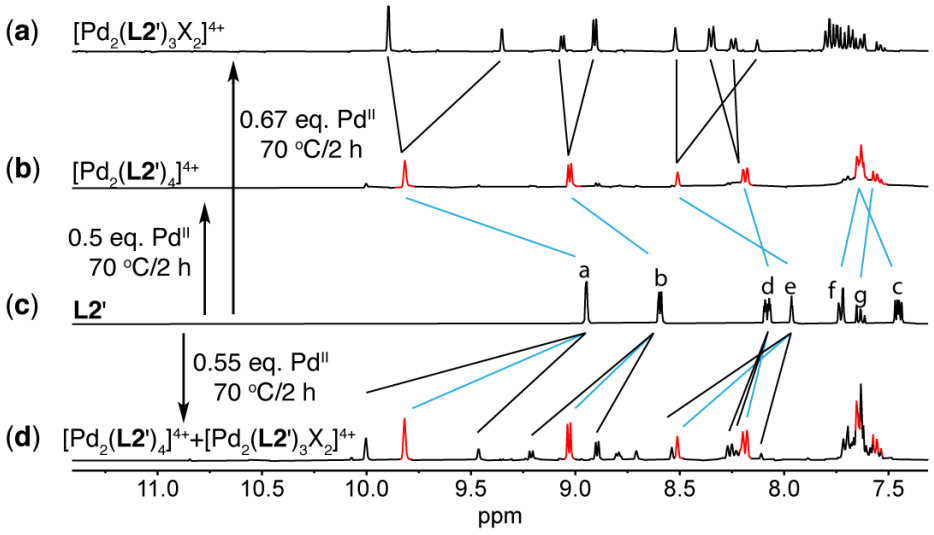

Figure S7. ^{1}H NMR spectra (400 MHz, CD_3CN) of **L2'** (c), $[Pd_2(\mathbf{L2'})_4](BF_4)_4$ (b), $[Pd_2(\mathbf{L2'})_3X_2](BF_4)_4$ (a) and a mixture of cage $[Pd_2(\mathbf{L2'})_4](BF_4)_4$ and bowl compound $[Pd_2(\mathbf{L2'})_3X_2](BF_4)_4$ (d).

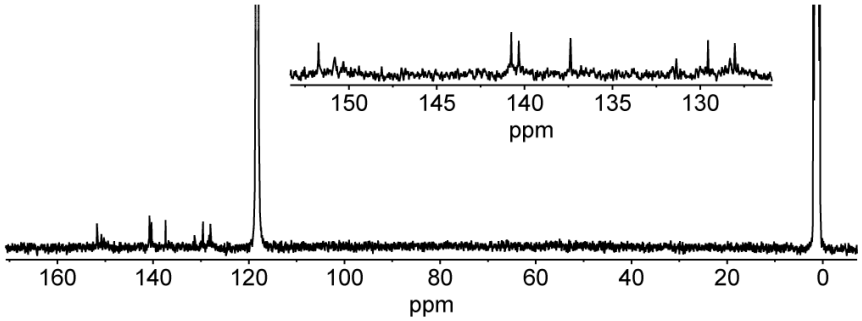

Figure S8. ^{13}C NMR spectra (101 MHz, CD_3CN) of $[Pd_2(\mathbf{L2'})_4](BF_4)_4$.

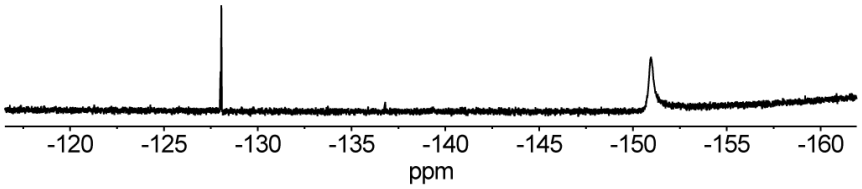

Figure S9. ^{19}F NMR spectrum (400 MHz, CD_3CN) of $[Pd_2(\mathbf{L2'})_4](BF_4)_4$. The signal at –128 ppm indicates encapsulation of BF_4^-. This signal disappears upon addition of NBu_4NO_3 (1 eq).

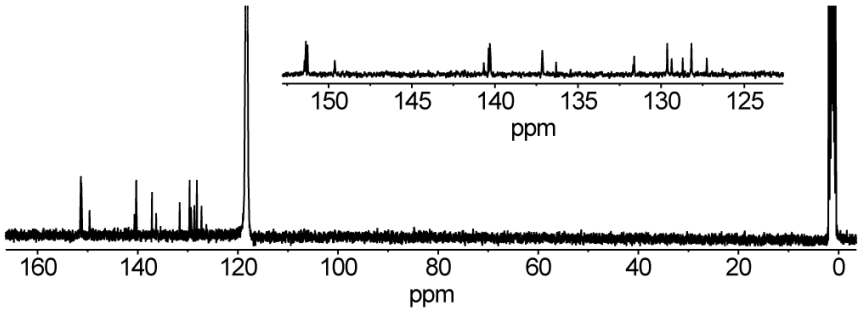

Figure S10. ^{13}C NMR spectra (101 MHz, CD_3CN) of $[Pd_2(\mathbf{L2'})_3X_2](BF_4)_4$.

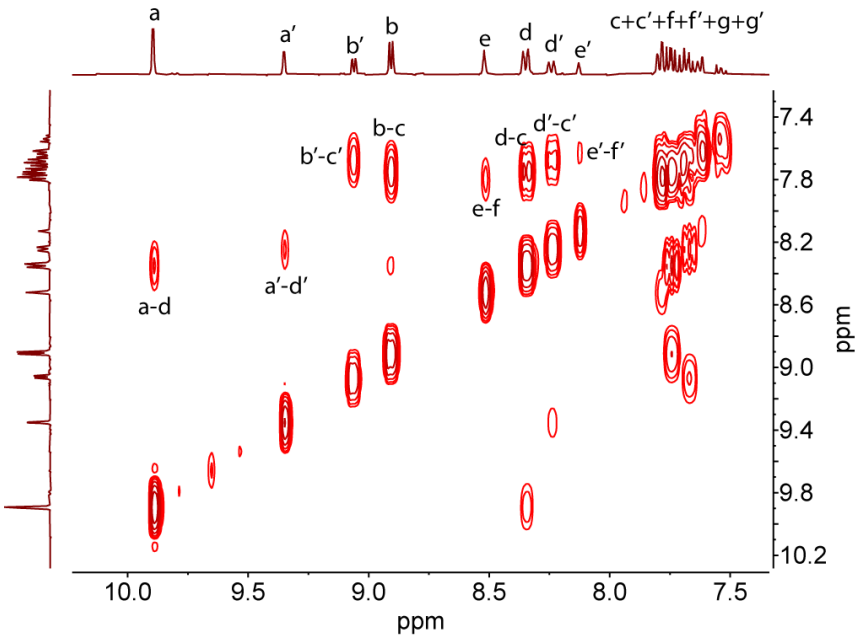

Figure S11. ^{1}H - ^{1}H COSY NMR spectrum (400 MHz, CD_3CN) of $[Pd_2(\mathbf{L2'})_3X_2](BF_4)_4$.

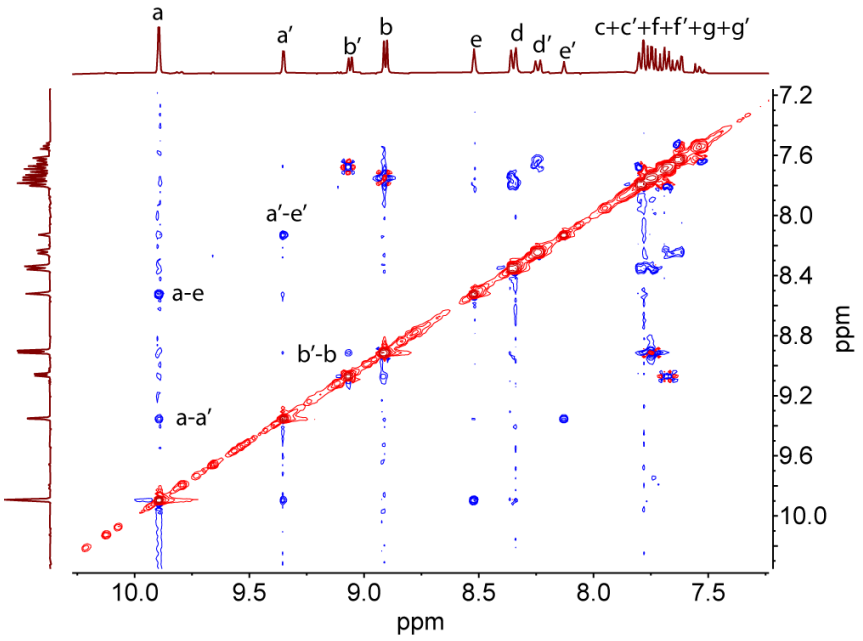

Figure S12. ^{1}H - ^{1}H NOESY NMR spectrum (400 MHz, CD_3CN) of $[Pd_2(\mathbf{L2'})_3X_2](BF_4)_4$.

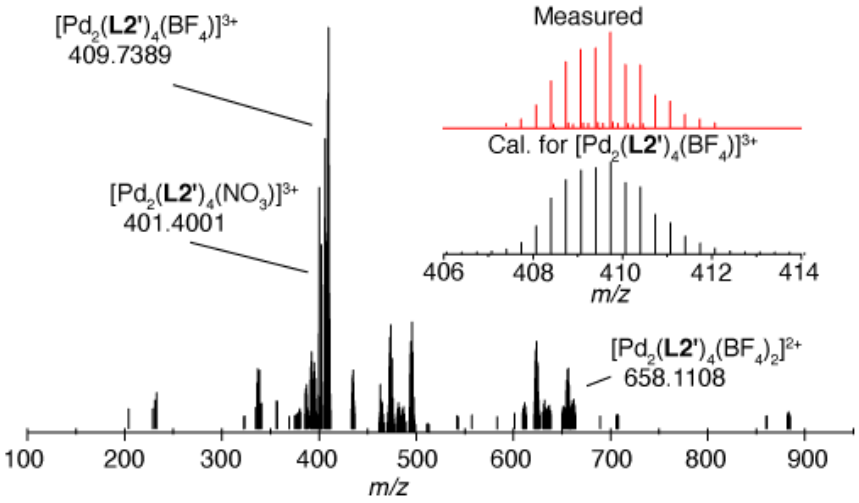

Figure S13. High-Resolution ESI Mass spectrum of cage $[Pd_2(\mathbf{L2'})_4](BF_4)_4$.

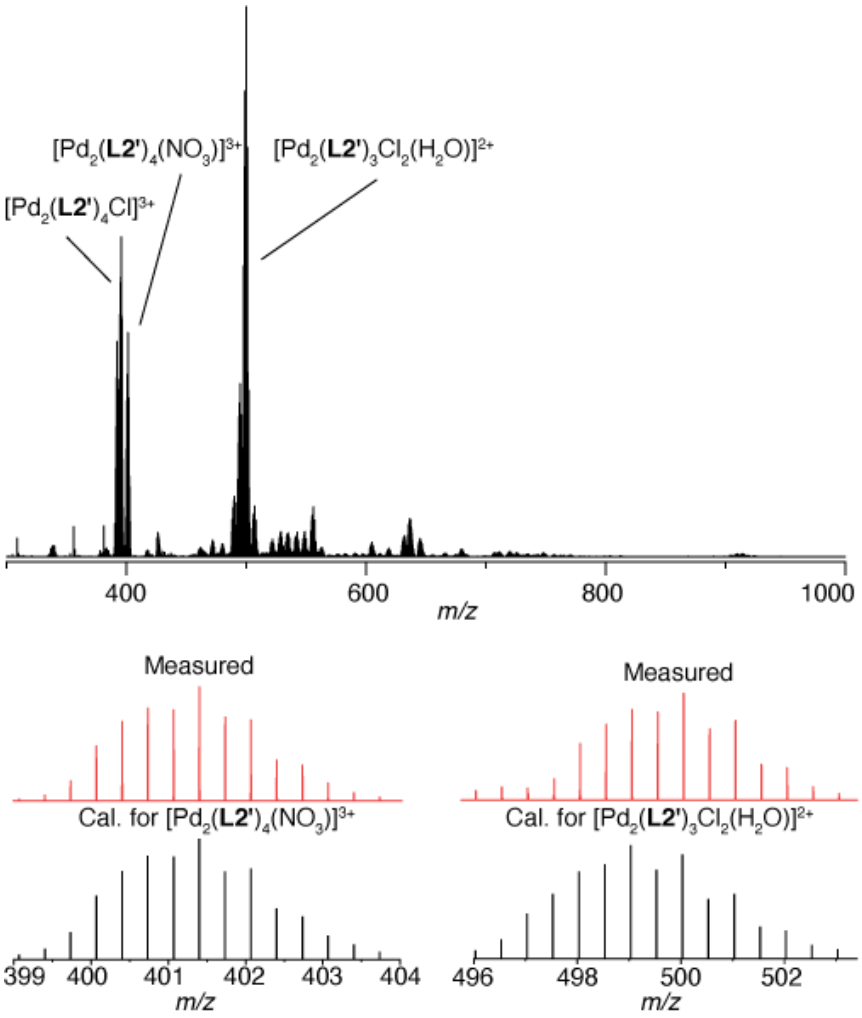

Figure S14. High-Resolution ESI Mass spectrum a mixture of cage $[Pd_2(\mathbf{L2'})_4](BF_4)_4$ and bowl $[Pd_2(\mathbf{L2'})_3X_2](BF_4)_4$.

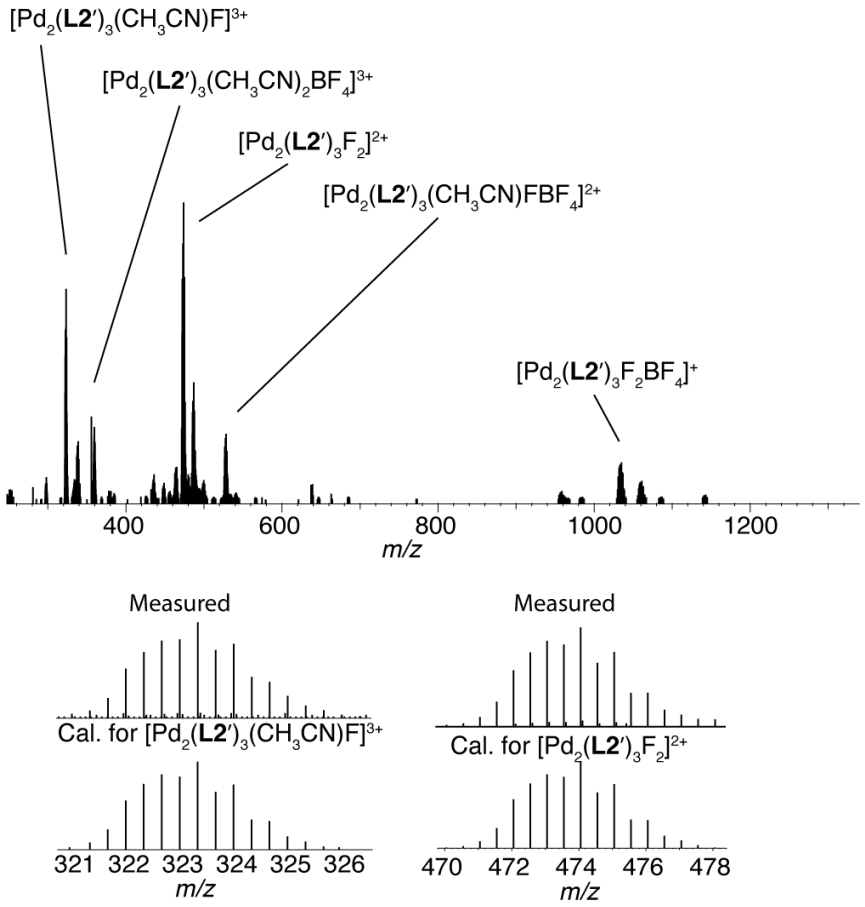

Figure S15. High-Resolution ESI Mass spectrum of the bowl $[Pd_2(\mathbf{L2'})_3X_2](BF_4)_4$.

2.2.2 Synthesis of $[Pd_2(\mathbf{L2'})_4](NO_3)_4$

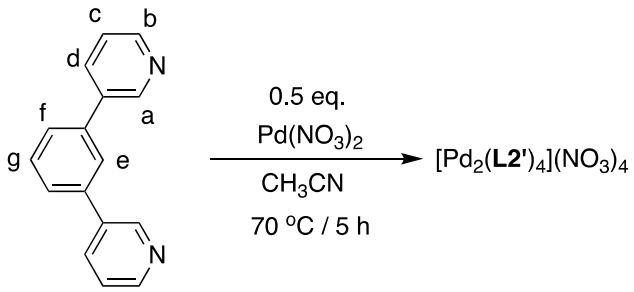

The cage compound $[Pd_2(\mathbf{L2'})_4](NO_3)_4$ was synthesized in quantitative yield by stiring a mixture of ligand **L2'** (9 μmol, 200 μL of a 45 mM stock solution of **L2'** in CD_3CN) and $Pd(NO_3)_2$ (4.5 μmol, 150 μL of a 30 mM stock solution in CD_3CN) in 650 μL CD_3CN at 70 °C for 5 h to give 1000 μL of a 2.25 mM solution of $[Pd_2(\mathbf{L2'})_4](NO_3)_4$. ^{1}H NMR (400 MHz, CD_3CN) δ 10.27 (d, J = 2.0 Hz, 8H), 9.42 (dd, J = 5.8, 1.3 Hz, 8H), 9.17 (t, J = 1.9 Hz, 4H), 8.26 (dt, J = 8.2, 1.6 Hz, 8H), 7.68 (td, J = 5.6, 2.9 Hz, 16H), 7.61 – 7.50 (m, 4H).

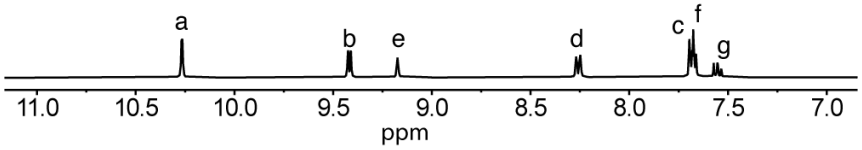

Figure S16. ^{1}H NMR (400 MHz, CD_3CN) spectrum of cage $[Pd_2(\mathbf{L2'})_4](NO_3)_4$ (only showing aromatic region).

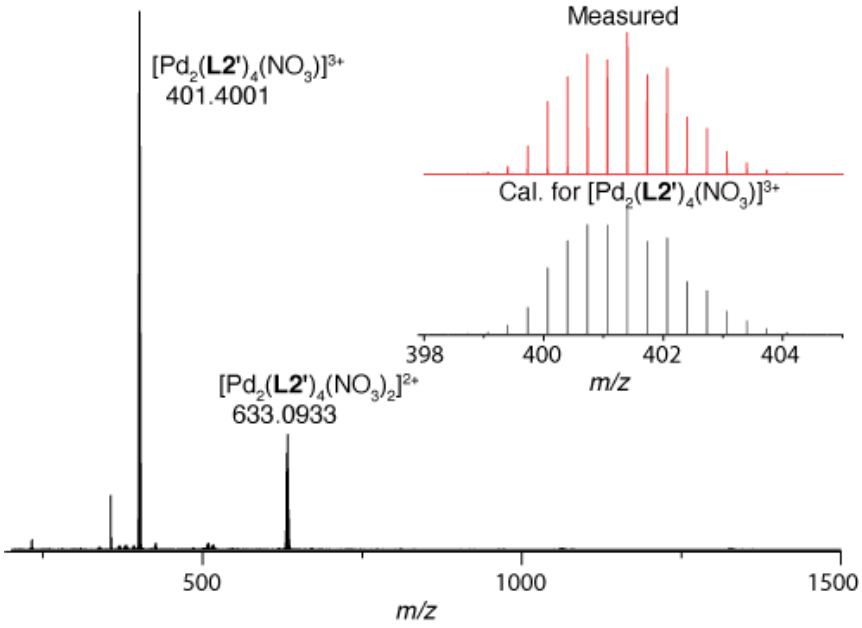

Figure S17. High-Resolution ESI Mass spectrum of cage $[Pd_2(\mathbf{L2'})_4](NO_3)_4$.

2.2.3 Synthesis of $[Pd_{12}(\mathbf{L3})_{24}](BF_4)_{24}$

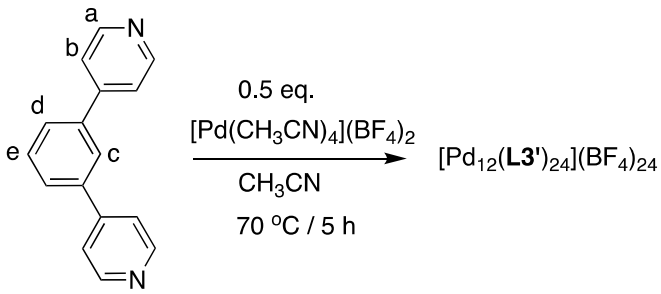

The cage compound $[Pd_{12}(\mathbf{L3'})_{24}](BF_4)_{24}$ was synthesized by stiring a mixture of ligand **L3'** (9 μmol, 200 μL of a 45 mM stock solution of **L3'** in CD_3CN) and $[Pd(CH_3CN)_4](BF_4)_2$ (4.5 μmol, 150 μL of a 30 mM stock solution in CD_3CN) in 650 μL CD_3CN at 70 °C for 5 h to give 1000 μL of a 0.375 mM solution of $[Pd_{12}(\mathbf{L3'})_{24}](BF_4)_{24}$. ^1H NMR (400 MHz, CD_3CN) δ 9.28 – 9.02 (m, 96H), 8.23 (s, 24H), 8.08 – 7.96 (m, 96H), 7.94 – 7.84 (m, 48H), 7.63 (t, J = 7.9 Hz, 24H).

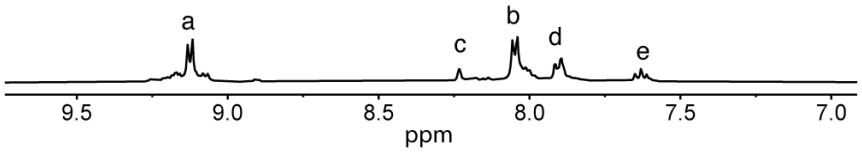

Figure S18. ^1H NMR (400 MHz, CD_3CN) spectrum of cage $[Pd_{12}(\mathbf{L3'})_{24}](BF_4)_{24}$ (only showing aromatic region).

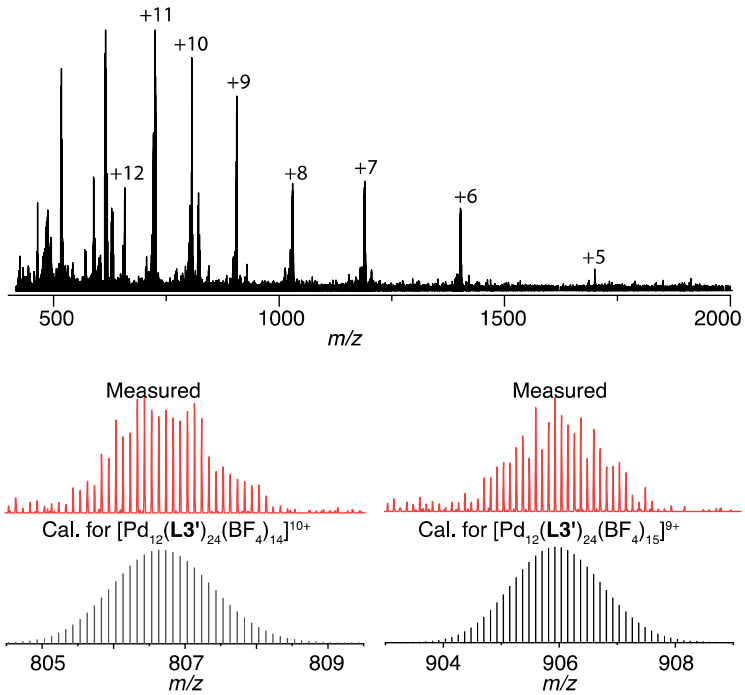

Figure S19. High-Resolution ESI Mass spectrum of cage $[Pd_{12}(\mathbf{L3'})_{24}](BF_4)_{24}$.

2.2.4 Synthesis of $[Pd_3(\mathbf{L4'})_6](BF_4)_6$ & $[Pd_4(\mathbf{L4'})_8](BF_4)_8$

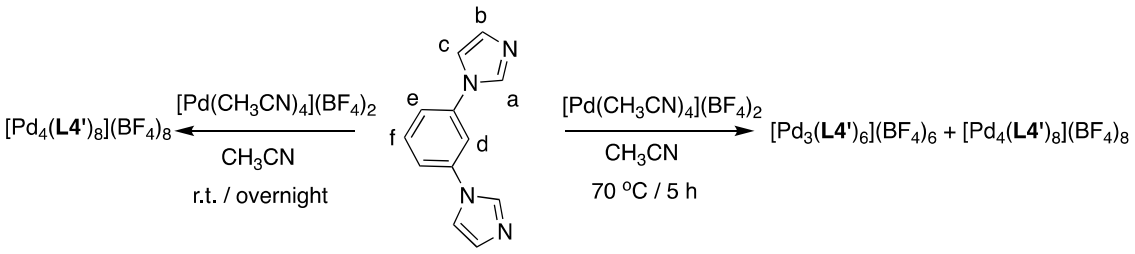

The cage compound $[Pd_4(\mathbf{L4'})_8](BF_4)_8$ was synthesized in quantitative yield by stiring a mixture of ligand **L4'** (9 µmol, 200 µL of a 45 mM stock solution of **L4'** in CD_3CN) and $[Pd(CH_3CN)_4](BF_4)_2$ (4.5 µmol, 150 µL of a 30 mM stock solution in CD_3CN) in 650 µL CD_3CN at room temperature overnight to give 1000 µL of a 1.125 mM solution of $[Pd_4(\mathbf{L4'})_8](BF_4)_8$. ^{1}H NMR (400 MHz, CD_3CN) δ 8.58 (s, 16H), 7.76 (s, 8H), 7.71 (t, J = 8.1 Hz, 8H), 7.60 (d, J = 1.3 Hz, 32H), 7.60 – 7.53 (m, 16H). The reaction of ligand **L4'** (9 µmol, 200 µL of a 45 mM stock solution of **L4'** in CD_3CN) with $[Pd(CH_3CN)_4](BF_4)_2$ (4.5 µmol, 150 µL of a 30 mM stock solution in CD_3CN) in 650 µL CD_3CN at 70 °C for 5 h, however, offered a mixture of $[Pd_4(\mathbf{L4'})_8](BF_4)_8$ and $[Pd_3(\mathbf{L4'})_6](BF_4)_6$.

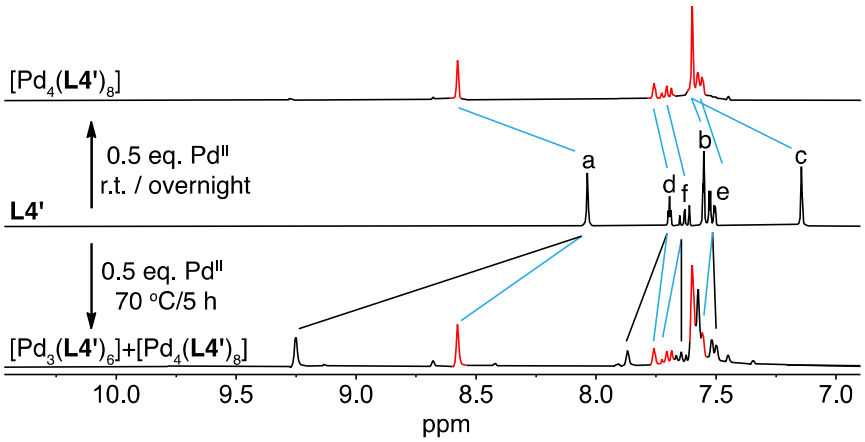

Figure S20. Aromatic region of the ^{1}H NMR spectra (400 MHz, CD_3CN) of **L4'** (middle), $[Pd_4(\mathbf{L4'})_8](BF_4)_8$ (top), and a mixture of cage $[Pd_3(\mathbf{L4'})_6](BF_4)_6$ and bowl compound $[Pd_4(\mathbf{L4'})_8](BF_4)_8$ (bottom). Since only one set of signals is observed for $[Pd_4(\mathbf{L4'})_8](BF_4)_8$, we proposed that the assembly has a macrocyclic structure (for a tetrahedral structure, two sets of ligand signals would be expected).

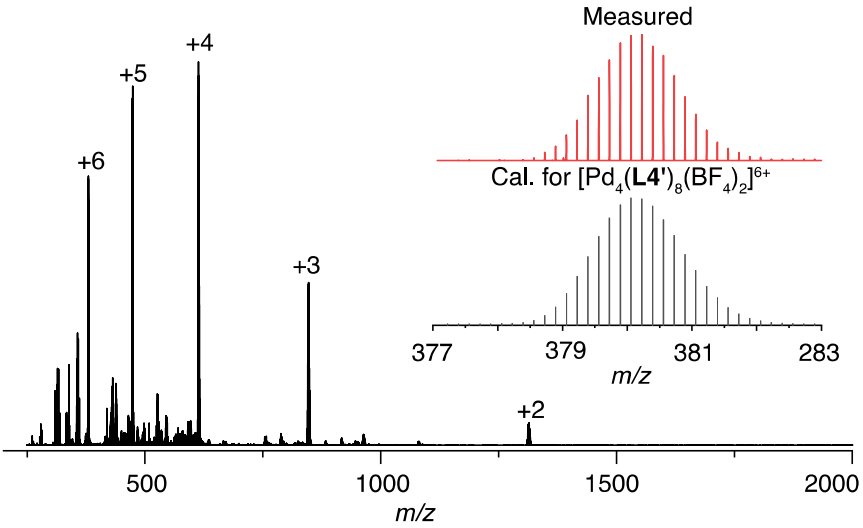

Figure S21. High-Resolution ESI Mass spectrum of cage $[Pd_4(\mathbf{L4'})_8](BF_4)_8$

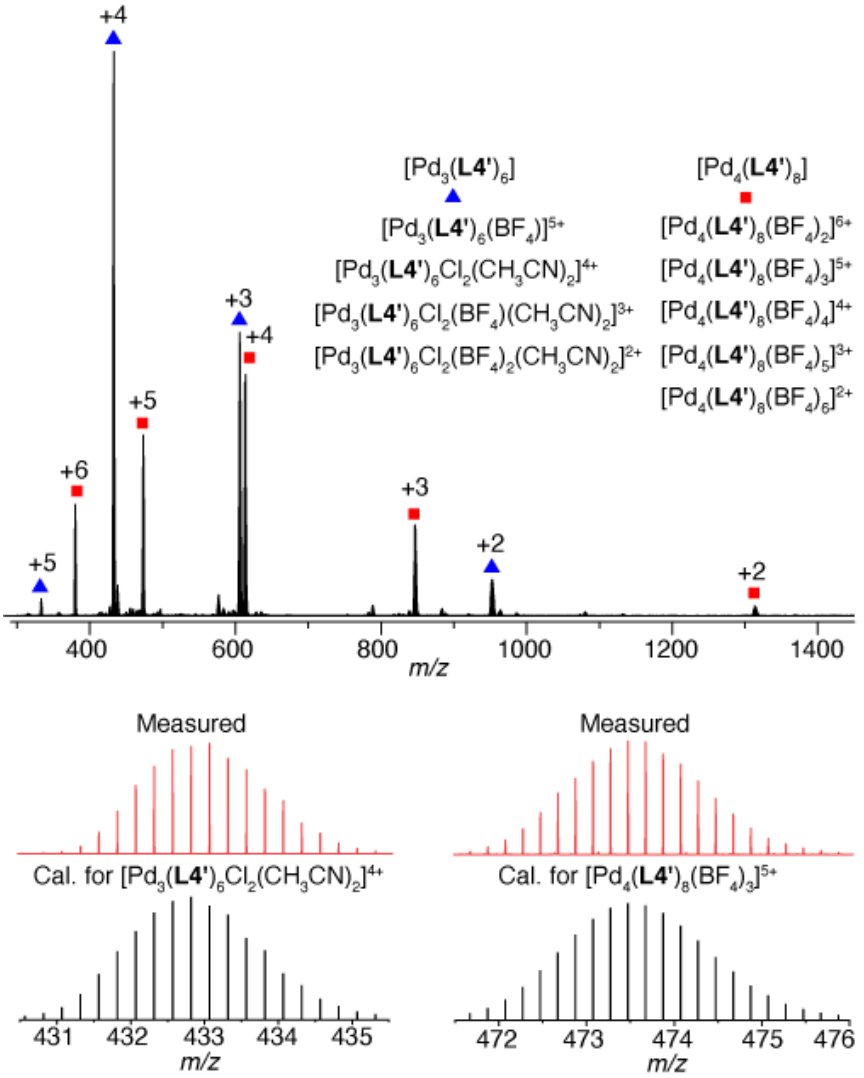

Figure S22. High-Resolution ESI Mass spectrum of a mixture of $[Pd_4(\mathbf{L4'})_8](BF_4)_8$ and $[Pd_3(\mathbf{L4'})_6](BF_4)_6$.

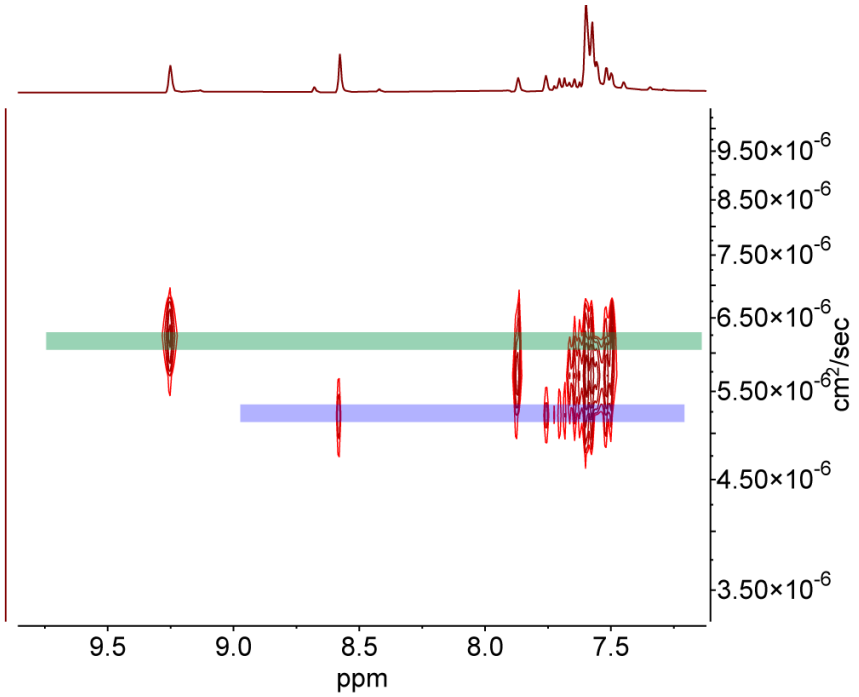

Figure S23. 1H-1H DOSY NMR (400 MHz, CD_3CN) spectrum of a mixture of $[Pd_4(\mathbf{L4'})_8](BF_4)_8$ (blue) and $[Pd_3(\mathbf{L4'})_6](BF_4)_6$ (green).

2.3 Synthesis of supramolecular polymer networks/gels

2.3.1 Synthesis of **P1**

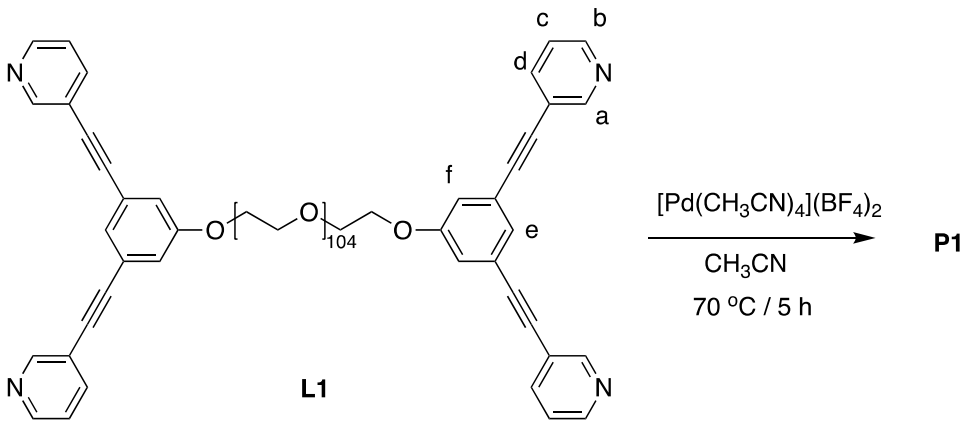

The supramolecular polymer network/gel $[Pd_2(\mathbf{L1})_2](BF_4)_4$ (**P1**) was prepared according to a modified literature procedure.[S9] In dilute solution, **P1** was synthesized by stiring a mixture of ligand **L1** (5 mg) and $[Pd(CH_3CN)_4](BF_4)_2$ (35 μL of a 30 mM stock solution in CD_3CN) in 500 μL CD_3CN at 70 °C for 3 h. ^{1}H NMR (400 MHz, CD_3CN, only showing the aromatic region) δ 9.41 (s), 9.07 (d, J = 5.9 Hz), 8.09 (d, J = 7.5 Hz), 7.65 (t, J = 7.1 Hz), 7.52 (s), 7.26 (s). The gel sample was made in a similar way but 4 times more concentrated: in a 1.5 mL vial, 20 mg of **L1** was dissolved with 460 μL CH_3CN, later 40 μL of a 100 mM $[Pd(CH_3CN)_4](BF_4)_2$ stock solution in CH_3CN was added. The mixture was vortexed till they were mixed well before it was annealed at 70 °C for 4 h to obtain gel **P1**.

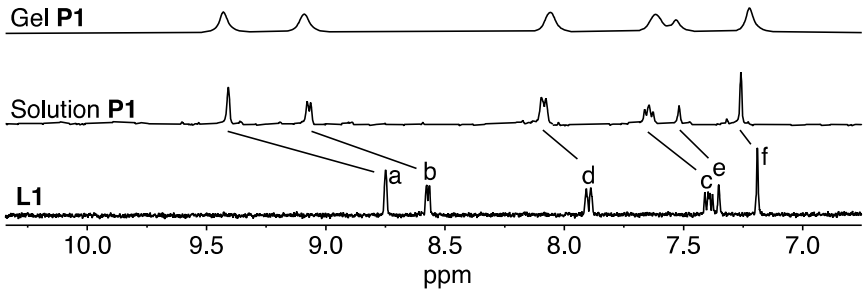

Figure S24. Aromatic region of the ^{1}H NMR spectra (400 MHz, CD_3CN) of **L1** (bottom), of a dilute solution of **P1** (middle), and ^{1}H MAS NMR spectrum of gel **P1** (top).

2.3.2 Synthesis of **P2**

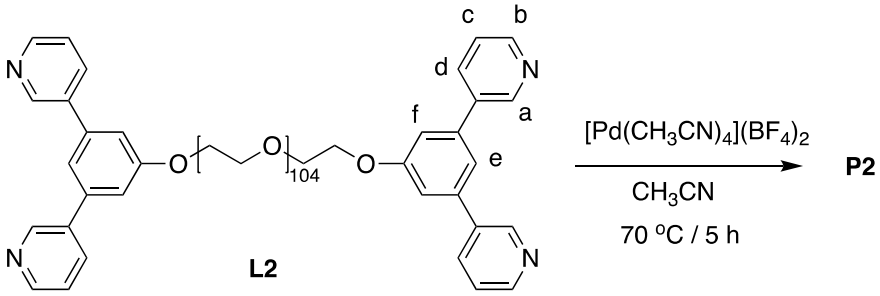

$[Pd_2(\mathbf{L2})_2](BF_4)_4$+$[Pd_2(\mathbf{L2})_{1.5}X_2](BF_4)_4$ (**P2**) in dilute solution was synthesized by stiring a mixture of ligand **L2** (5 mg) and $[Pd(CH_3CN)_4](BF_4)_2$ (35 μL of a 30 mM stock solution in CD_3CN) in 500 μL CD_3CN at 70 ºC for 5 h. The gel sample was made in an analogous fashion as **P1**: in a 1.5 mL vial, 20 mg of **L2** was dissolved with 460 μL CH_3CN, later 40 μL of a 100 mM $[Pd(CH_3CN)_4](BF_4)_2$ stock solution in CH_3CN was added. The mixture was vortexed till they were mixed well before it was annealed at 70 °C for 5 h to obtain gel **P2**.

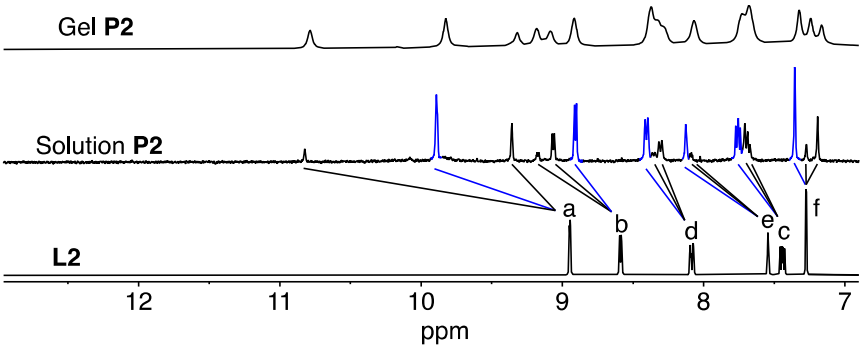

Figure S25. Aromatic region of the ^{1}H NMR spectra (400 MHz, CD_3CN) of **L2** (bottom), of a dilute solution of **P2** (middle, blue color representing $[Pd_2L_4]$), and ^{1}H MAS NMR spectrum of gel **P2** (top).

2.3.3 Synthesis of **P3**

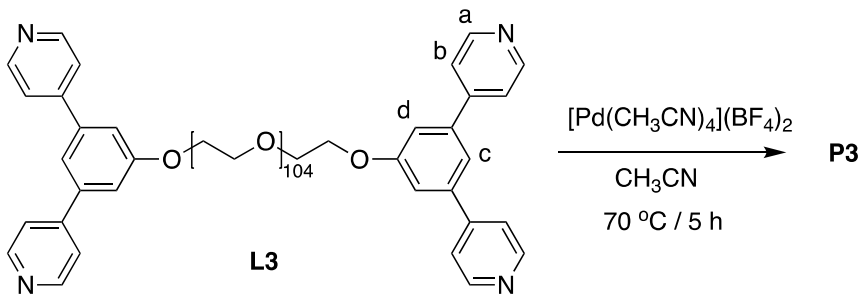

$[Pd_{12}(\mathbf{L3})_{12}](BF_4)_{24}$ (**P3**) in dilute solution was synthesized by stiring a mixture of ligand **L3** (5 mg) and $[Pd(CH_3CN)_4](BF_4)_2$ (35 μL of a 30 mM stock solution in CD_3CN) in 500 μL CD_3CN at 70 ºC for 5 h. The gel sample was made in an analogous fashion as **P1**: in a 1.5 mL vial, 20 mg of **L3** was dissolved with 460 μL CH_3CN, later 40 μL of a 100 mM $[Pd(CH_3CN)_4](BF_4)_2$ stock solution in CH_3CN was added. The mixture was vortexed till they were mixed well before it was annealed at 70 °C for 5 h to obtain gel **P3**.

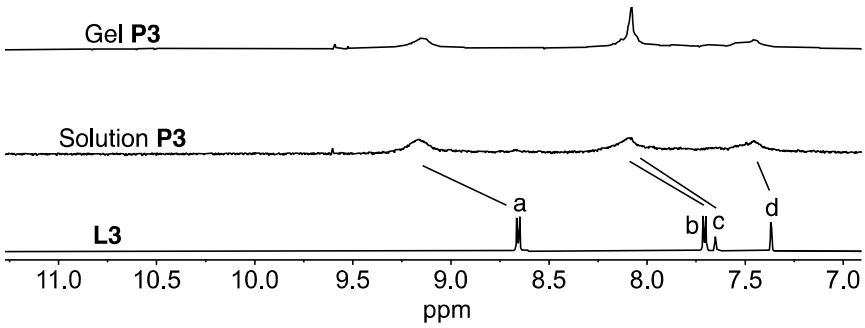

Figure S26. Aromatic region of the ^1H NMR spectra (400 MHz, CD_3CN) of **L3** (bottom), of a dilute solution of **P3** (middle), and ^1H MAS NMR spectrum of gel **P3** (top).

2.3.4 Synthesis of **P4**

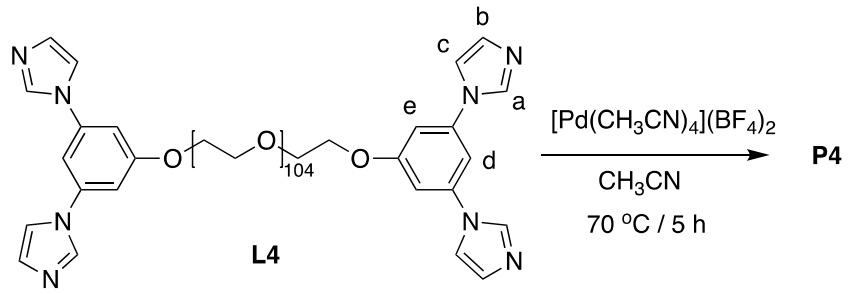

$[Pd_3(\mathbf{L4})_3](BF_4)_6$+$[Pd_4(\mathbf{L4})_4](BF_4)_8$ (**P4**) in dilute solution was synthesized by stiring a mixture of ligand **L4** (1 μmol, 5.1 mg) and $[Pd(CH_3CN)_4](BF_4)_2$ (1.05 μmol, 35 μL of a 30 mM stock solution in CD_3CN) in 500 μL CD_3CN at 70 °C for 5 h. The gel sample was made in an analogous fashion as **P1**: in a 1.5 mL vial, 20 mg of **L4** was dissolved with 460 μL CH_3CN, later 40 μL of a 100 mM $[Pd(CH_3CN)_4](BF_4)_2$ stock solution in CH_3CN was added. The mixture was vortexed till they were mixed well before it was annealed at 70 °C for 5 h to obtain gel **P4**.

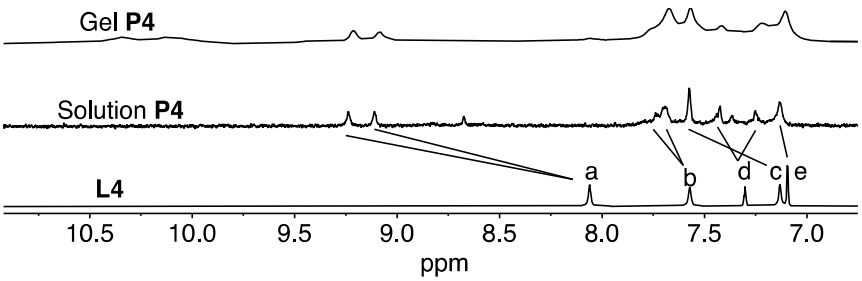

Figure S27. Aromatic region of the ^{1}H NMR spectra (400 MHz, CD_3CN) of **L4** (bottom), of a dilute solution of **P4** (middle), and ^{1}H MAS NMR spectrum of gel **P4** (top).

3 Photoacid

3.1 Synthesis of photoacid **PAH'**(BF_4)

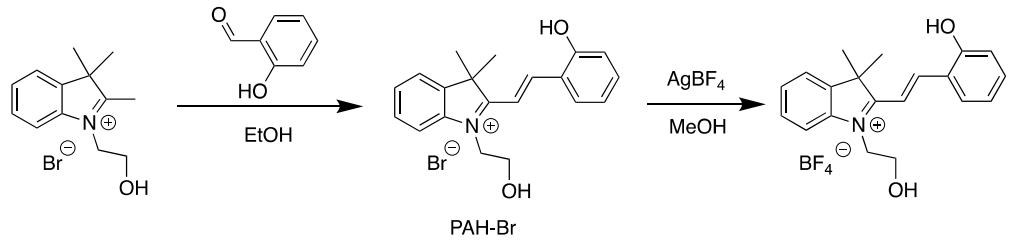

PAH-Br

In a 50-mL round-bottom flask, 1-(2-hydroxyethyl)-2,3,3-trimethyl-3H-indolium bromide (1.0 g, 3.5 mmol) was dissolved in absolute EtOH (10 mL). Salicylaldehyde (0.65 g, 5.3 mmol) was added, the flask sealed with a septum, and the solution degassed by gentle N_2 bubbling (10 min) prior to heating it up to 100 °C under stirring (250 rpm) overnight. The resulting orange precipitate was filtered, washed with EtOH (3 × 10 mL) to remove unreacted materials, and recrystallized from hot MeOH. Slow overnight cooling to 4 °C resulted in the formation of orange crystals (PAH-Br), which were collected, washed with cold MeOH, and dried under vacuum (0.5 g, 37%). ^{1}H NMR (400 MHz, DMSO) δ 11.02 (s, 1H), 8.55 (d, *J* = 16.5 Hz, 1H), 8.11 (dd, *J* = 8.0, 1.7 Hz, 1H), 7.96 – 7.90 (m, 1H), 7.90 – 7.85 (m, 1H), 7.80 (d, *J* = 16.5 Hz, 1H), 7.67 – 7.57 (m, 2H), 7.47 (ddd, *J* = 8.5, 7.1, 1.6 Hz, 1H), 7.06 (dd, *J* = 8.3, 1.1 Hz, 1H), 7.03 – 6.94 (m, 1H), 4.75 (t, *J* = 5.0 Hz, 2H), 3.91 (t, *J* = 5.0 Hz, 2H), 1.79 (s, 6H). ^{13}C NMR (101 MHz, d_6-DMSO) δ 183.16, 158.88, 148.18, 143.42, 141.08, 135.42, 129.86, 129.08, 128.94, 122.93, 121.29, 119.92, 116.72, 115.43, 112.63, 58.50, 52.05, 49.36, 26.48.

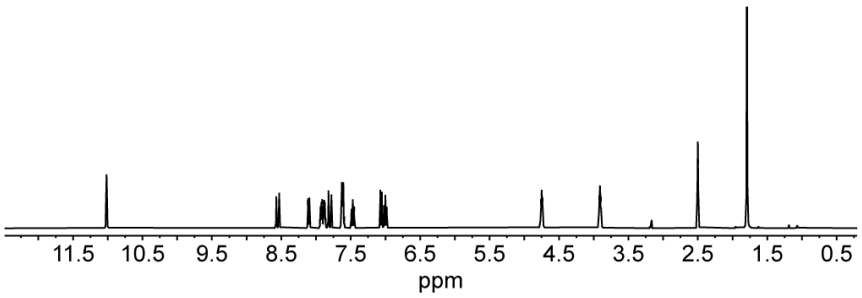

Figure S28. ^{1}H NMR (400 MHz, d_6-DMSO) spectrum of PAH-Br.

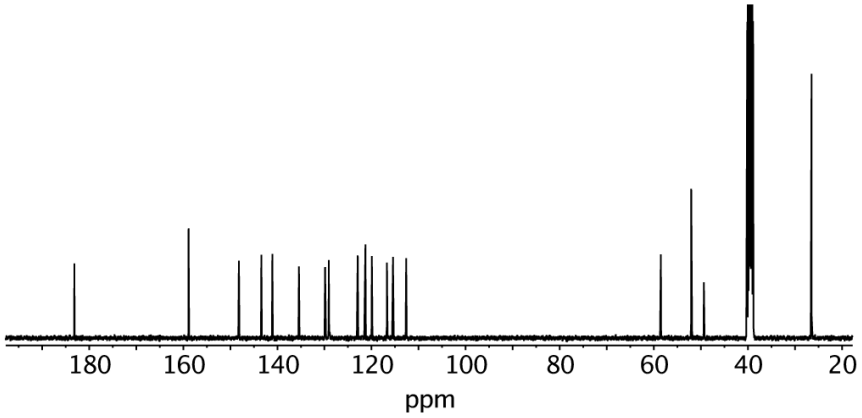

Figure S29. ^{13}C NMR (101 MHz, d_6-DMSO) spectrum of PAH-Br.

Subsequently, PAH-Br (100 mg, 0.26 mmol) was dissolved in MeOH (5 mL). A solution of $AgBF_4$ (50 mg, 0.26 mmol, 1 eq.) in MeOH (200 µL) was added in order to exchange the Br^- anion for BF_4^-. After stirring the mixture at room temperature for 30 min, the solid precipitate was removed by filtration, and the the solution was concentrated under reduced pressure, resulting in the formation of an orange powder, **PAH'**(BF_4), which was isolated by filtration and dried under vacuum (95 mg, 93%). ^{1}H NMR (400 MHz, CD_3CN) δ 8.58 (d, *J* = 16.4 Hz, 1H), 8.27 (s, 1H), 7.88 (dd, *J* = 8.2, 1.7 Hz, 1H), 7.77 – 7.66 (m, 2H), 7.63 (d, *J* = 4.1 Hz, 1H), 7.62 – 7.56 (m, 2H), 7.49 (ddd, *J* = 8.5, 7.3, 1.6 Hz, 1H), 7.11 – 7.00 (m, 2H), 4.60 (t, *J* = 5.1 Hz, 2H), 4.03 (q, *J* = 5.4 Hz, 2H), 3.32 (t, *J* = 5.8 Hz, 1H), 1.81 (s, 6H). ^{13}C NMR (101 MHz, CD_3CN) δ 185.00, 159.16, 150.34, 144.47, 142.09, 136.49, 130.85, 130.51, 130.15, 123.78, 122.36, 121.89, 117.59, 116.11, 113.70, 59.80, 53.48, 50.33, 27.07. ESI-MS: *m/z* calculated for $C_{20}H_{22}NO_2$ $[M–BF4]^+$ 308.16, found 308.16.

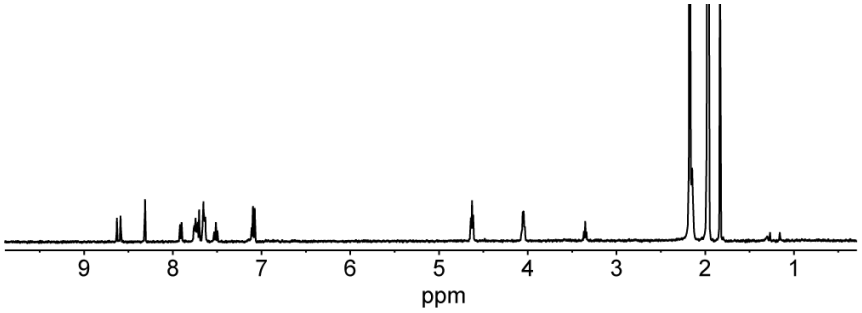

Figure S30. ^{1}H NMR (400 MHz, CD_3CN) spectrum of **PAH'**(BF_4).

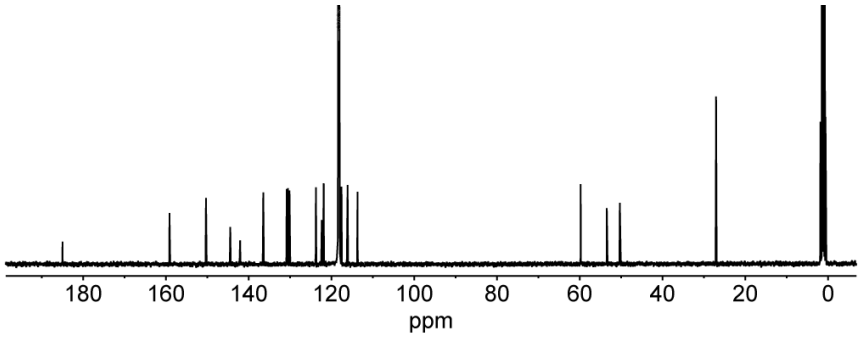

Figure S31. ^{13}C NMR (101 MHz, CD_3CN) spectrum of **PAH'**(BF_4).

3.2 Photoswitching

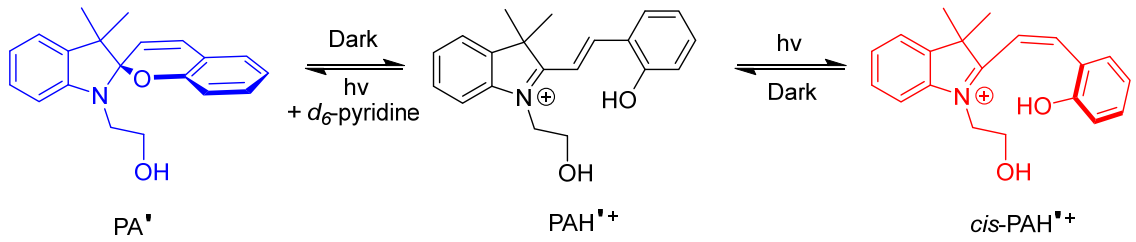

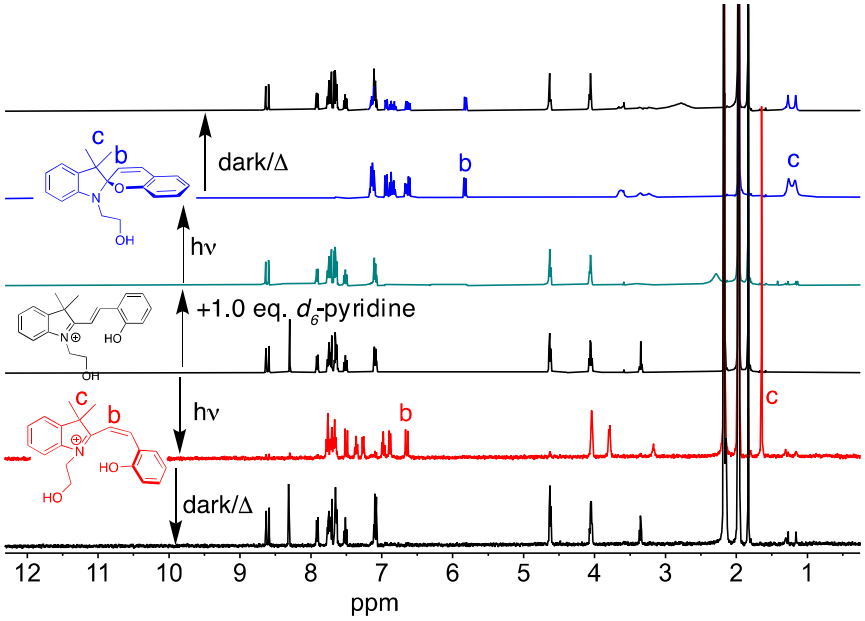

Figure S32. ^{1}H NMR spectra (400 MHz, CD_3CN) showing the photoswitching behavior of **PAH**$^{\bullet+}$ in the presence and in the absence of d_6-pyridine. Ring-closure to the spiropyran form is only observed in the presence of pyridine.

4 Determination of the relative ligand basicity

The relative basicity of the ligands **L1'**–**L4'** and **L5** was determined by NMR titration experiments. Two ligands (4.5 µmol, 9 mM for the ligands) were combined in CD_3CN (0.5 mL). A stock solution of TFA (57.4 µL in 1 mL CD_3CN, 750 mM) was prepared to contain 4.5 µmol TFA per 6 µL stock solution. Per sample there was 2 x 4.5 µmol of ditopic ligands (36 mM of pyridine groups) present. With the addition of 6 µL TFA stock solution (9 mM), 0.25 eq. of the total amount of pyridine groups were protonated.

For every combination, there were 6 points recorded, with the last point being 1.25 eq. of acid (45 mM) per pyridine group (36 mM) present in solution. The plots below show the average chemical shifts of multiple selected signals for each ligand in the mixture with respect to the normalized chemical shift at 1.25 eq. of acid (normalized to 100%).

The ligand basicity was found to increase in the order: **L1'** < **L2'** ~ **L3'** < **L4'** < **L5**

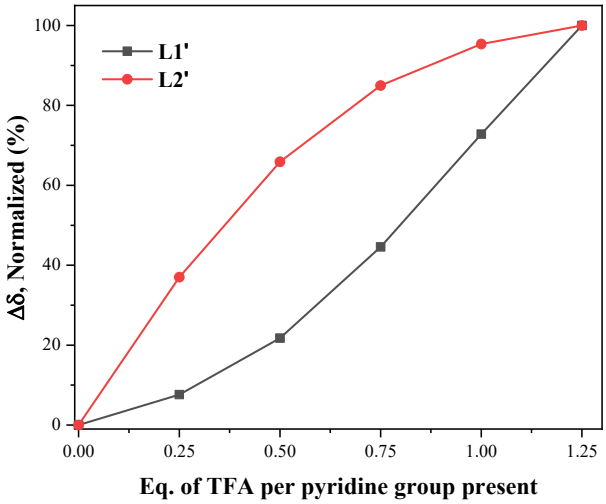

Figure S33. Variations of the ^{1}H NMR (400 MHz, CD_3CN) signals of ligand **L1'** and **L2'** upon addition of increasing amounts of TFA. The titration was performed in CD_3CN with [**L1'**] = 9 mM and [**L2'**] = 9 mM. The differences in chemical shifts are normalized with the maximum shift set to 100 %. Averaged values of 2 or 3 different signals are given.

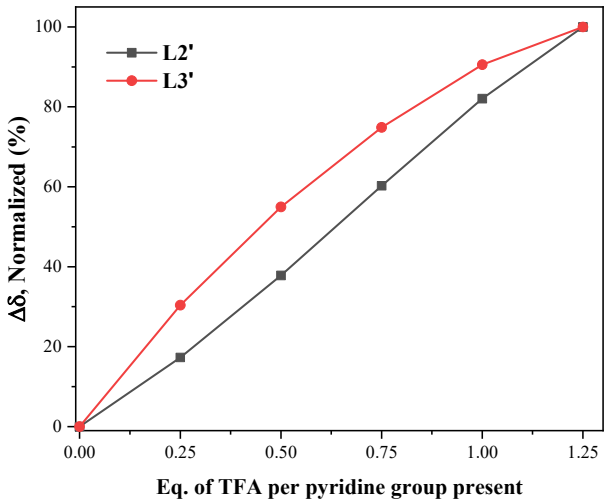

Figure S34. Variations of the ^{1}H NMR (400 MHz, CD_3CN) signals of ligand **L2'** and **L3'** upon addition of increasing amounts of TFA. The titration was performed in CD_3CN with [**L2'**] = 9 mM and [**L3'**] = 9 mM. The differences in chemical shifts are normalized with the maximum shift set to 100 %. Averaged values of 2 or 3 different signals are given.

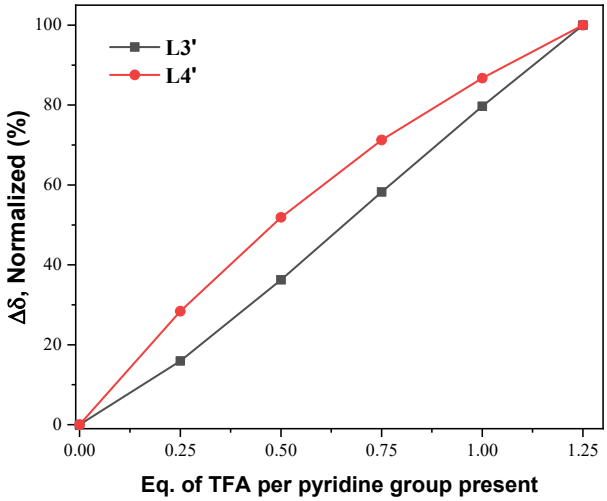

Figure S35. Variations of the ^{1}H NMR (400 MHz, CD_3CN) signals of ligand **L3'** and **L4'** upon addition of increasing amounts of TFA. The titration was performed in CD_3CN with [**L3'**] = 9 mM and [**L4'**] = 9 mM. The differences in chemical shifts are normalized with the maximum shift set to 100 %. Averaged values of 2 or 3 different signals are given.

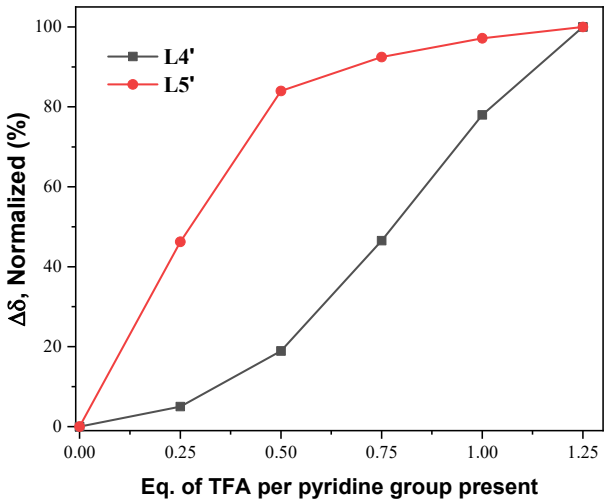

Figure S36. Variations of the ^{1}H NMR (400 MHz, CD_3CN) signals of ligand **L4'** and **L5** upon addition of increasing amounts of TFA. The titration was performed in CD_3CN:DCM 1:1 with [**L4'**] = 9 mM and [**L5**] = 9 mM. The differences in chemical shifts are normalized with the maximum shift set to 100 %. Averaged values of 2 or 3 different signals are given.

5 Determination of the Huynh electronic parameter (HEP)

The respective ditopic ligand (4.5 μmol, 9 mM) and the dimeric carbene complex $[PdBr_2(iPr_2\text{-bimy})]_2$ (4.2 mg, 4.5 μmol, 9 mM) were combined in $CDCl_3$ (0.5 mL). The ^1H and ^{13}C spectra were recorded directly after mixing. The residual solvent signal from $CDCl_3$ is referenced to 77.7 ppm,.

Table S1. The Huynh electronic parameters of the ligands [ppm].

	L1'[S11]	**L2'**	**L3'**	**L4'**	**L5**[S11]
HEP	159.4	159.8	160.0	160.7	161.4

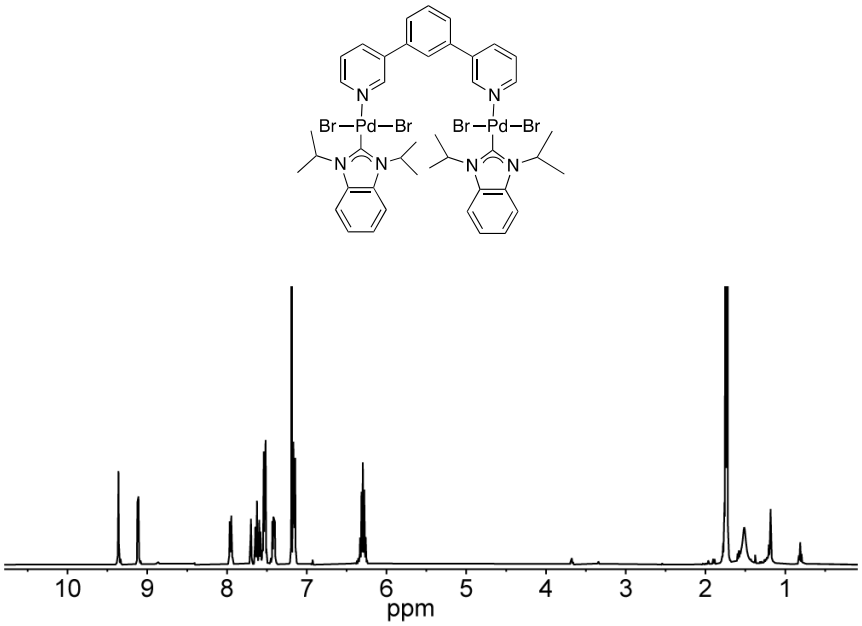

Figure S37. ^1H NMR (400 MHz, $CDCl_3$) spectrum of **HEP-L2'** complex.

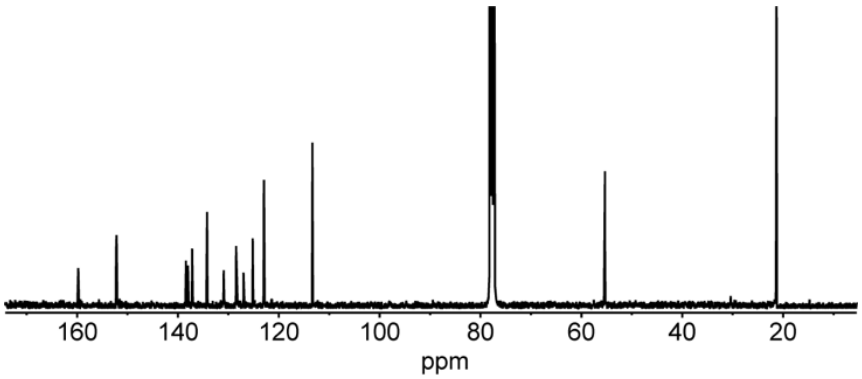

Figure S38. ^{13}C NMR (101 MHz, $CDCl_3$) spectrum of **HEP-L2'** complex.

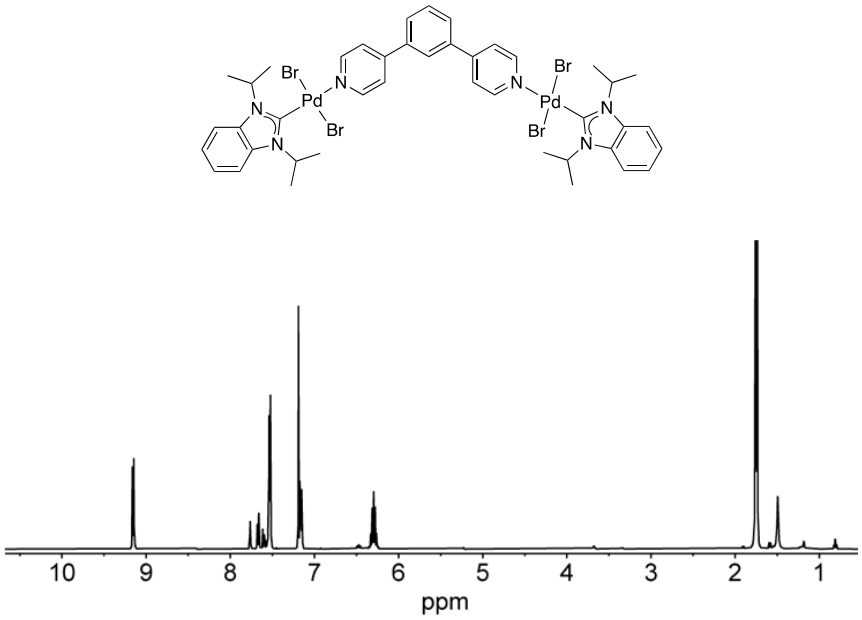

Figure S39. ^{1}H NMR (400 MHz, $CDCl_3$) spectrum of **HEP-L3'** complex.

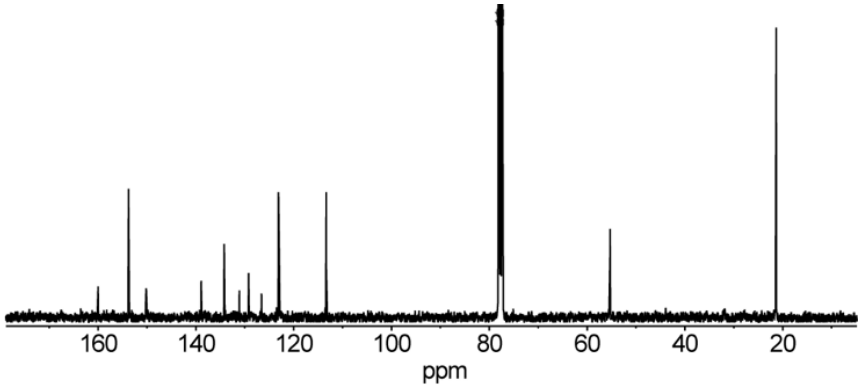

Figure S40. ^{13}C NMR (101 MHz, $CDCl_3$) spectrum of **HEP-L3'** complex.

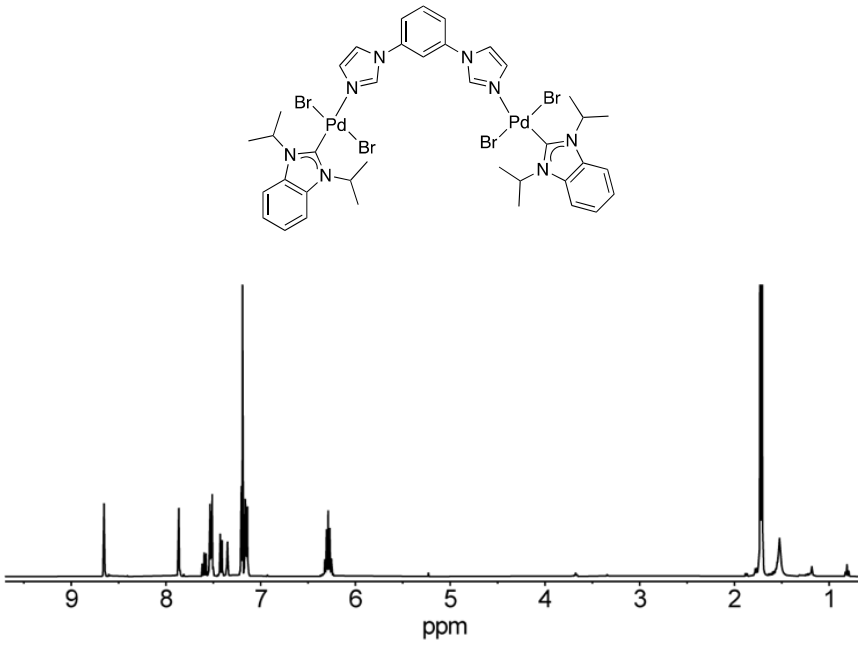

Figure S41. ^{1}H NMR (400 MHz, $CDCl_3$) spectrum of **HEP-L4'** complex.

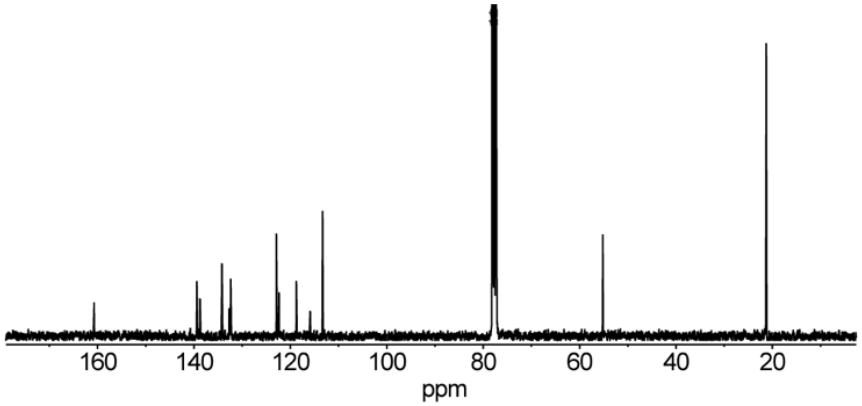

Figure S42. ^{13}C NMR (101 MHz, $CDCl_3$) spectrum of **HEP-L4'** complex.

6 Acid-induced disassembly of Pd-based polymer networks

The gels were prepared as described in section 2. An aliquot (85.3 µL) of a stock solution of TFA in CH_3CN (750 mM) was added to the respective gel sample, and the mixture was vortexed. Subsequently, the mixture was heated to 70 °C for 2 h. A gel-sol conversion was observed for **P2**–**P4**, whereas the gel state of **P1** was maintained (Figure S43). The difference can be explained by the lower basicity of **L1**, when compared to **L2**–**L4**, which renders **P1** more resistant to acid.

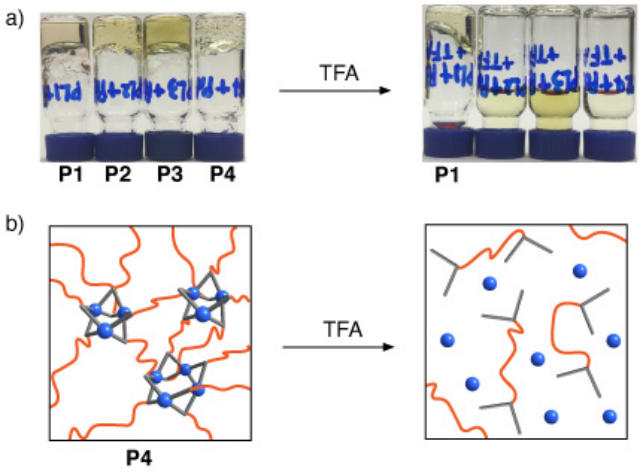

Figure S43. a) TFA-induced gel-sol conversion of **P2**–**P4**; b) Schematic representation of the disassembly of **P4**.

7. Light-induced disassembly of Pd-based polymer networks

The gels were prepared as described in section 2. The photoacid **PAH'**(BF_4) (6.3 mg, 16 µmol) was added to the respective gel sample, and the mixture was vortexed. Upon irradiation with blue light at RT for 2 h, a gel-sol conversion was observed for **P2**–**P4**, whereas the gel state of **P1** was maintained (Figure S44). A reverse sol-gel conversion could be induced by heating the solutions in the absence of light at 70 °C for 2 h. The switch between gel and solution state could be repeated five times.

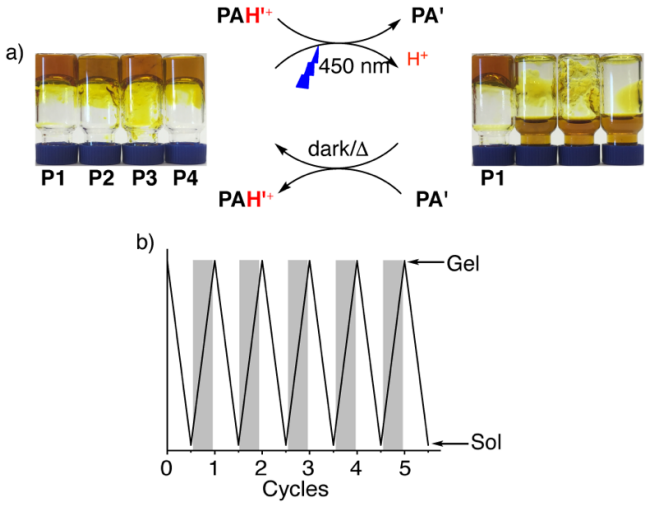

Figure S44. a) Light-induced disassembly of Pd-based polymer networks; b) Reversible sol-gel conversion of **P2**–**P4** for 5 cycles.

8 Acid-induced assembly of a Pd-based polymer network

An aliquot (40 µL) of a stock solution of $[Pd(CH_3CN)_4](BF_4)_2$ in CH_3CN (100 mM) was added to a suspension of polymer ligand **L1** (20 mg, ~4.0 µmol) and metalloligand **L5** (5.2 mg, 8.0 µmol) in CH_3CN (0.45 mL). Upon heating the suspension at 70 °C for 2 h, a clear orange solution was obtained. **L5** is poorly soluble in CH_3CN, and its dissolution indicates that a reaction with Pd^{2+} had taken place. An aliquot (85.3 µL) of a stock solution of TFA in CH_3CN (750 mM) was added to the solution, and the mixture was heated to 70 °C for 6 h. A sol-gel conversion was observed as evidenced by the vial inversion test (Figure S45).

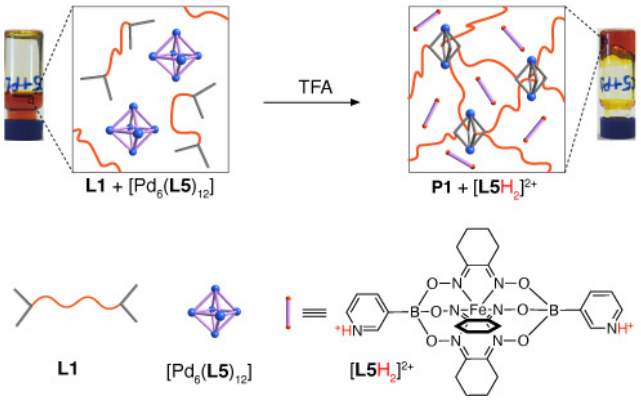

Figure S45. TFA-induced conversion of a mixture of $[Pd_6(\mathbf{L5})_{12}](BF_4)_{12}$ and **L1** into **P1** and $[\mathbf{L5}H_2]^{2+}$.

In order to monitor the process by ^{1}H NMR spectroscopy, we performed a similar experiment with lower concentrations. An aliquot (33.4 µL) of a stock solution of $[Pd(CH_3CN)_4](BF_4)_2$ in CH_3CN (30 mM) was added to a suspension of polymer ligand **L1** (5 mg, ~1.0 µmol) and metalloligand **L5** (1.3 mg, 2.0 µmol) in CH_3CN (0.5 mL). After heating the mixture at 70 °C for 2 h, a ^{1}H NMR spectrum was recorded. An aliquot (21.3 µL) of a stock solution of TFA in CH_3CN (750 mM) was added to the solution, and the mixture was heated to 70 °C for 2 h. Subsequently, another ^{1}H NMR spectrum was recorded (Figure S46).

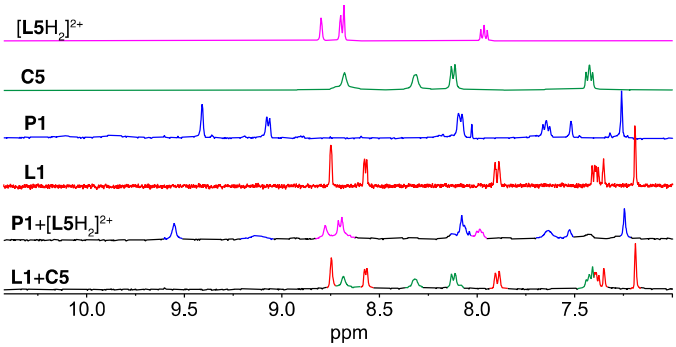

Figure S46. Aromatic region of the ^{1}H NMR spectra (400 MHz, CD_3CN) of a mixture of $[Pd(CH_3CN)_4](BF_4)_2$ (1 eq.), ligand **L1** (2 eq.), and ligand **L5** (2 eq.) before (spectrum on the bottom) and after (spectrum directly above) addition of the TFA. The relevant reference spectra are shown above (red: **L1**, green: **C5** ('cage 5') = $[Pd_6(\mathbf{L5})_{12}]^{12+}$, blue: **P1**, purple: $[\mathbf{L5}H_2]^{2+}$).

9 Light-induced sol-gel and gel-sol conversions

9.1 Light-induced assembly of a Pd-based polymer network

An aliquot (60 µL) of a stock solution of $[Pd(CH_3CN)_4](BF_4)_2$ in CH_3CN (100 mM) was added to a suspension of polymer ligand **L1** (30 mg, ~6.0 µmol) and metalloligand **L5** (7.8 mg, 12 µmol) in CH_3CN (0.45 mL). Upon heating the suspension at 70 °C for 2 h, a clear orange solution was obtained. Next, the photoacid **PAH'**(BF_4) (19 mg, 48 µmol) was added, and the mixture was irradiated with blue light at 50 °C for 11 h. A sol-gel conversion was observed as evidenced by the vial inversion test (Figure S47). A reverse gel-sol conversion could be induced by heating the gel in the absence of light at 70 °C for 7 h. The cycle could be repeated four times.

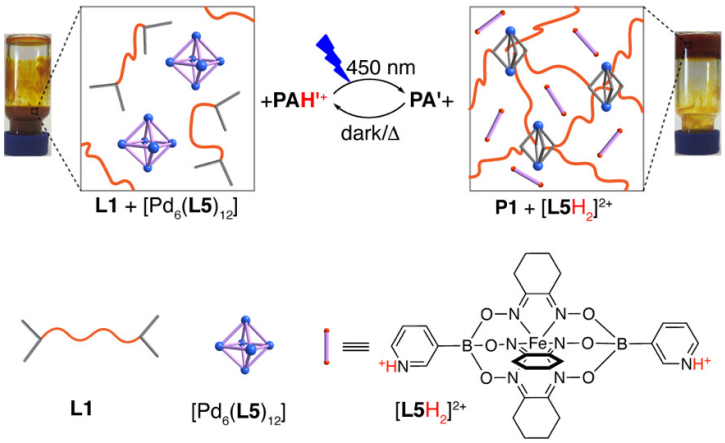

Figure S47. Light-induced conversion of $[Pd_6(\mathbf{L5})_{12}](BF_4)_{12}$ and **L1** into **P1** and $[\mathbf{L5}H_2]^{2+}$.

In order to monitor the process by ^{1}H NMR spectroscopy, we performed a similar experiment with lower concentrations. An aliquot (33.4 µL) of a stock solution of $[Pd(CH_3CN)_4](BF_4)_2$ in CH_3CN (30 mM) was added to a suspension of polymer ligand **L1** (5 mg, ~1.0 µmol) and metalloligand **L5** (1.3 mg, 2.0 µmol) in CH_3CN (0.5 mL). After heating the mixture at 70 °C for 2 h, the photoacid **PAH'**(BF_4) (3.16 mg, 8 µmol) was added, and a ^{1}H NMR spectrum was recorded. The mixture was then irradiated with blue light at 50 °C for 7 h, and a second ^{1}H NMR spectrum was recorded. The sample was then kept in the dark at 70 °C for 5 h, before recording another spectrum. The irradiation/tempering-in-the-dark cycle was repeated another four times (Figure S48).

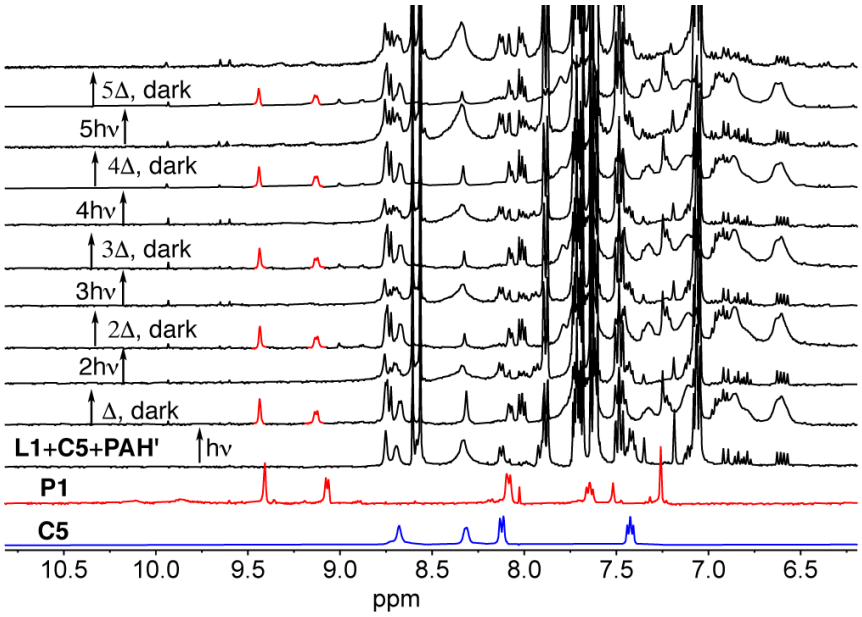

Figure S48. Aromatic part of the ^{1}H NMR spectra (400 MHz, CD_3CN) of a solution containing $[Pd_6(\mathbf{L5})_{12}](BF_4)_{12}$ (= **C5**; 'cage 5'), **L1**, and **PAH'**(BF_4). The sample was repeatedly irradiated and then tempered in the dark. The relevant reference spectra of $\mathbf{P1}_{dilute}$ (red) and **C5** (blue) are given at the bottom.

9.2 Light-induced conversion of polymer network **P3** into cage $[Pd_2(\mathbf{L1'})_4](BF_4)_4$

In order to corroborate the importance of the ligand basicity for the switching process, we have also examined the light-induced conversion of **P3** into cage $[Pd_2(\mathbf{L1'})_4](BF_4)_4$ (ligand basicity: **L3** > **L1'**).

An aliquot (40 µL) of a stock solution of $[Pd(CH_3CN)_4](BF_4)_2$ in CH_3CN (100 mM) was added to a solution of polymer ligand **L3** (20 mg, ~4.0 µmol) and ligand **L1'** (2.2 mg, 8 µmol) in CH_3CN (0.45 mL). Gelation was observed immediately. After vortexing for one minute, the mixture was annealed at 70 °C for 5 h. Next, the photoacid **PAH'**(BF_4) (12.6 mg, 32 µmol) was added, and the mixture was vortexed. Irradiation with blue light at RT for 2 h resulted in a gel-sol conversion (Figure S49). A reverse sol-gel conversion could be induced by heating the gel in the absence of light at 70 °C for 2 h. The cycle could be repeated four times.

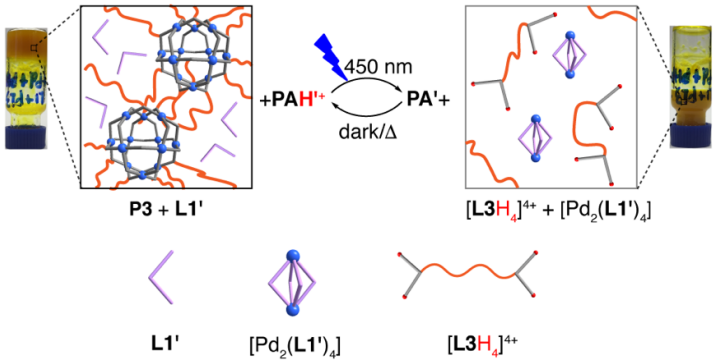

Figure S49. Light-induced of conversion of polymer network **P3** into cage $[Pd_2(\mathbf{L1'})_4](BF_4)_4$.

In order to monitor the process by ^{1}H NMR spectroscopy, we performed a similar experiment with lower concentrations. An aliquot (33.4 µL) of a stock solution of $[Pd(CH_3CN)_4](BF_4)_2$ in CH_3CN (30 mM) was added to a suspension of polymer ligand **L3** (5 mg, ~1.0 µmol) and ligand **L1'** (0.55 mg, 2.0 µmol) in CH_3CN (0.5 mL). After heating the mixture at 70 °C for 5 h, the photoacid **PAH'**(BF_4) (3.16 mg, 8 µmol) was added, and a ^{1}H NMR spectrum was recorded. The mixture was then irradiated with blue light at RT for 7 h, and a second ^{1}H NMR spectrum was recorded. The sample was then kept in the dark at 70 °C for 5 h, before recording another spectrum. The irradiation/tempering-in-the-dark cycle was repeated another four times (Figure S50).

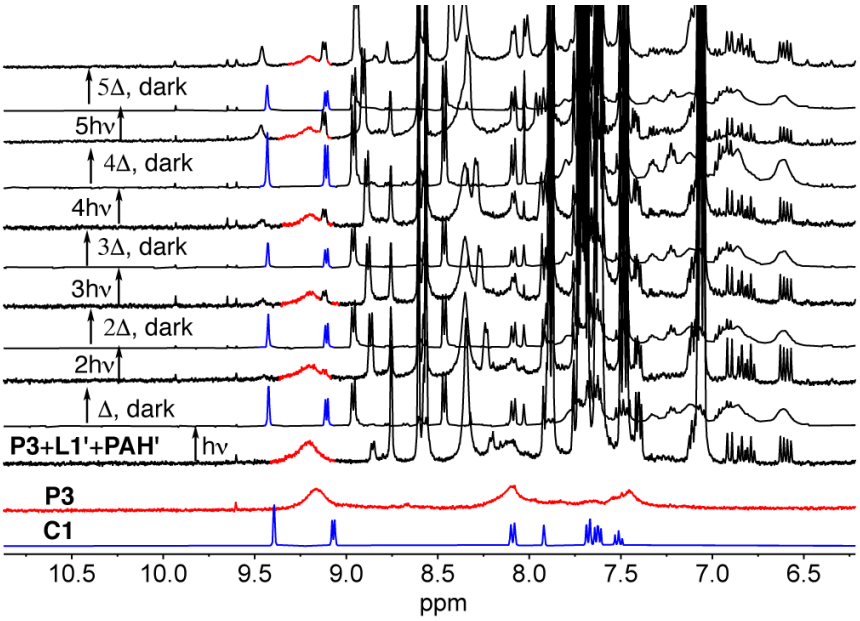

Figure S50. Aromatic part of the ^{1}H NMR spectra (400 MHz, CD_3CN) of a solution containing **P3**$_{dilute}$, **L1'**, and **PAH'**(BF_4). The sample was repeatedly irradiated and then tempered in the dark. The relevant reference spectra of **P3**$_{dilute}$ (red) and **C1** ('cage 1' = [Pd_2(**L1'**)$_4$](BF_4)$_4$, blue) are given at the bottom.

10 SEM images of gels

SEM images were obtained in GeminiSEM 300 Scanning Electron Microscope (Figure S51). The gel sample were spread directly on a silicon wafer, and then the samples were dried at RT before the SEM measurements were performed.

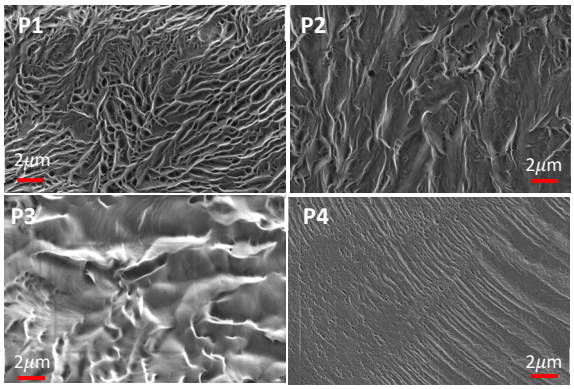

Figure S51. SEM images of **P1**, **P2**, **P3**, and **P4**.

11 References

S1 P. Liao, B. W. Langloss, A. M. Johnson, E. R. Knudsen, F. S. Tham, R. R. Julian and R. J. Hooley, *Chem. Commun.*, 2010, **46**, 4932–4934.

S2 B. Avitia, E. MacIntosh, S. Muhia and E. Kelson, *Tetrahedron Lett.*, 2011, **52**, 1631–1634.

S3 L. Zeng, Y. Xiao, J. Jiang, H. Fang, Z. Ke, L. Chen, and J. Zhang, *Inorg. Chem*., 2019, **58**, 10019−10027.

S4 D. Samanta and P. S. Mukherjee, *Chem. - Eur. J.*, 2014, **20**, 12483–12492.

S5 M. D. Wise, A. Ruggi, M. Pascu, R. Scopelliti and K. Severin, *Chem. Sci.*, 2013, **4**, 1658–1662.

S6 A. Schmidt, V. Molano, M. Hollering, A. Poethig, A. Casini and F. Kühn, *Chem. Eur. J*., 2016, **22**, 2253–2256.

S7 Y. Wang, M. Zhong, J. V. Park, A. V. Zhukhovitskiy, W. Shi and J. A. Johnson, *J. Am. Chem. Soc*., 2016, **138**, 10708–10715.

S8 H. V. Huynh, Y. Han, J. H. H. Ho and G. K. Tan, O*rganometallics*, 2006, **25**, 3267–3274.

S9 Y. Gu, E. A. Alt, H. Wang, X. Li, A. P. Willard and J. A. Johnson, *Nature*, 2018, **560**, 65–69.

S10 L. Baumann, K. Schoeller, D. Courten, D. Marti, M. Frenz, M. Wolf, R. M. Rossi, and L. J. Scherer, *RSC Adv.*, 2013, **3**, 23317–23326.

S11 S. M. Jansze and K. Severin, *J. Am. Chem. Soc*., 2019, **141**, 815–819.